Quantification of Cytokine Production and Intracellular Cytokine Analysis

For quantification of cytokines, $CD4^+$ T cells were purified from freshly prepared LPLs by staining with FITC-labeled anti-CD4 mAb (BD PharMingen) followed by flow cytometry with a FACS Vantage system. The purified $CD4^+$ T cells were added to wells of plates coated with anti-CD3 mAb (10 μg/ml, clone 145–2C11; BD PharMingen) and cultured in RPMI 1640 supplemented with 10% fetal calf serum (FCS), sodium pyruvate, L-glutamine, HEPES, and 50 μmol/L 2-mercaptoethanol (complete medium). Cultures were incubated for 48 hours at 37°C in 5% CO_2 in a moist air incubator. Cells in culture were removed, separated by centrifugation, and the supernatants were then subjected to a cytokine-specific ELISA, as described previously.[43] Briefly, microtiter plates were coated with mAbs to individual cytokines and blocked with 3% BSA in PBS at 37°C for 2 hours, and then diluted samples were added to well and incubated overnight at 4°C. Captured cytokines were detected using biotinylated detection mAbs and peroxidase-labeled anti-biotin mAb (Vector Laboratories Inc., Burlingame, CA). The following mAbs were used for coating and detection, respectively: anti-IFN-γ, R4-6A2 and XMG 1.2; anti-IL-2, JES6-1A12 and JES6-5H4 mAbs; anti-IL-4, BVD4-1D11 and BVD6-23G2. For intracellular cytokine analysis, LPLs were cultured in plates coated with anti-CD3 mAb in complete medium with anti-CD28 mAb. After 48 hours of culture, the cells were subjected to intracellular cytokine staining as described previously.[45] In brief, cells were stained with FITC-labeled anti-CD4 mAb (BD PharMingen), fixed, permealized, and then stained with PE-labeled anti-IFN-γ mAb (BD PharMingen) for analysis using flow cytometry.

Treatment with Antibiotics and Bacterial Culture

In some experiments, recipient mice were given a combination of antibiotics in their drinking water. Metronidazole (0.6 g/L, Wako Pure Chemical Industries Ltd.), neomycin (0.35 g/L, Wako), streptomycin (0.2 g/L, Wako), and bacitracin (0.35 g/L, Wako) were added to the drinking water, and the mice were continuously given this water *ad libitum* until the histological and cytological analyses were performed. To determine total colony forming units (CFU), mice were treated with antibiotics as above for 6 weeks, fasted for 6 hours and then the entire stomach was removed, washed three times with PBS, minced and homogenized with 2 ml of PBS in a Teflon-glass homogenizer. This homogenate was then subjected to serial dilution and spread over culture plates. Anaerobic bacteria were cultured on GAM agar plates (Nissui Pharmaceuticals, Tokyo, Japan) in culture jars (GasPack System BBL, Becton Dickinson) with AneroPac (Mitsubishi Gas Chemical Co, Inc., Tokyo, Japan). For aerobic cultures, brain-heart infusion agar (Difco, Becton Dickinson), chocolate agar, and sheep blood agar plates (both from Nissui) were used. To examine for the presence of indigenous microflora in the oral cavity, the mucosal surfaces of oral cavity were swabbed, and the swabs were placed in 300 μl of PBS. Then 100 μl of this suspension was spread over a culture plate. Anaerobic cultures were initiated within 20 minutes after taking samples. After 24 hours of incubation at 37°C, numbers of CFU were enumerated.

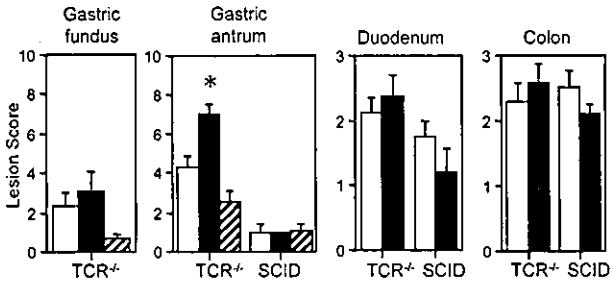

Figure 1. Histological scores of gastritis, duodenitis and colitis. $TCR^{-/-}$ or SCID mouse recipients were given RB^{Hi} T cells prepared from splenocytes of wt (**blank column**, $n = 8$), $IL\text{-}4^{-/-}$ (**solid column**, $n = 10$) or $IFN\text{-}\gamma^{-/-}$ (**hatched column**, $n = 7$) mice. The results shown are the mean and SEM. *, Difference between wt and $IFN\text{-}\gamma^{-/-}$ mice was statistically significant.

Statistics

The results were compared by the Mann-Whitney test using the Statview II statistical program (Abacus Concepts, Berkeley, CA) adapted for Macintosh computers. The results were considered to be statistically significant if P values were less than 0.05.

Results

Inflammation of the GI Tract in $TCR^{-/-}$ and SCID Mouse Recipients

Previous studies have shown that the transfer of RB^{Hi} T cells resulted in severe colitis in either SCID or $RAG^{-/-}$ mouse recipients, and the colitis was mediated by $CD4^+$ Th1-type cells.[4–6,9,46] A similar type of colitis was induced in $TCR^{-/-}$ recipients of wt RB^{Hi} T cells. Recipients of $IL\text{-}4^{-/-}$ RB^{Hi} T cells also developed a severe colitis (Figure 1). We noted that $TCR^{-/-}$ recipients of either wt or $IL\text{-}4^{-/-}$ RB^{Hi} T cells developed a duodenitis with a heavy cell infiltration, which was rarely described in SCID recipients previously. These changes were limited to the duodenum within 5 cm of the pylorus, and both the jejunum and ileum remained normal. We also found that these mouse recipients developed an inflammation of the stomach, especially in the antral region. When recipients of wt, $IL\text{-}4^{-/-}$, or $IFN\text{-}\gamma^{-/-}$ RB^{Hi} T cells were compared, recipients of $IL\text{-}4^{-/-}$ T cells developed the most severe gastritis and those mice receiving $IFN\text{-}\gamma^{-/-}$ T cells showed only minimal changes (Figure 1). Interestingly, SCID recipients of either wt or $IL\text{-}4^{-/-}$ RB^{Hi} T cells showed mild lesions in the stomach, with only slight cell infiltration. Adoptive transfer of wt or $IL\text{-}4^{-/-}$ $CD45RB^{low}$ T cells did not result in gastritis, duodenitis, or colitis (data not shown).

Pathological Features of Gastritis

In all 10 $TCR^{-/-}$ recipients of $IL\text{-}4^{-/-}$ RB^{Hi} T cells, the gastric antral and duodenal mucosa were increased in

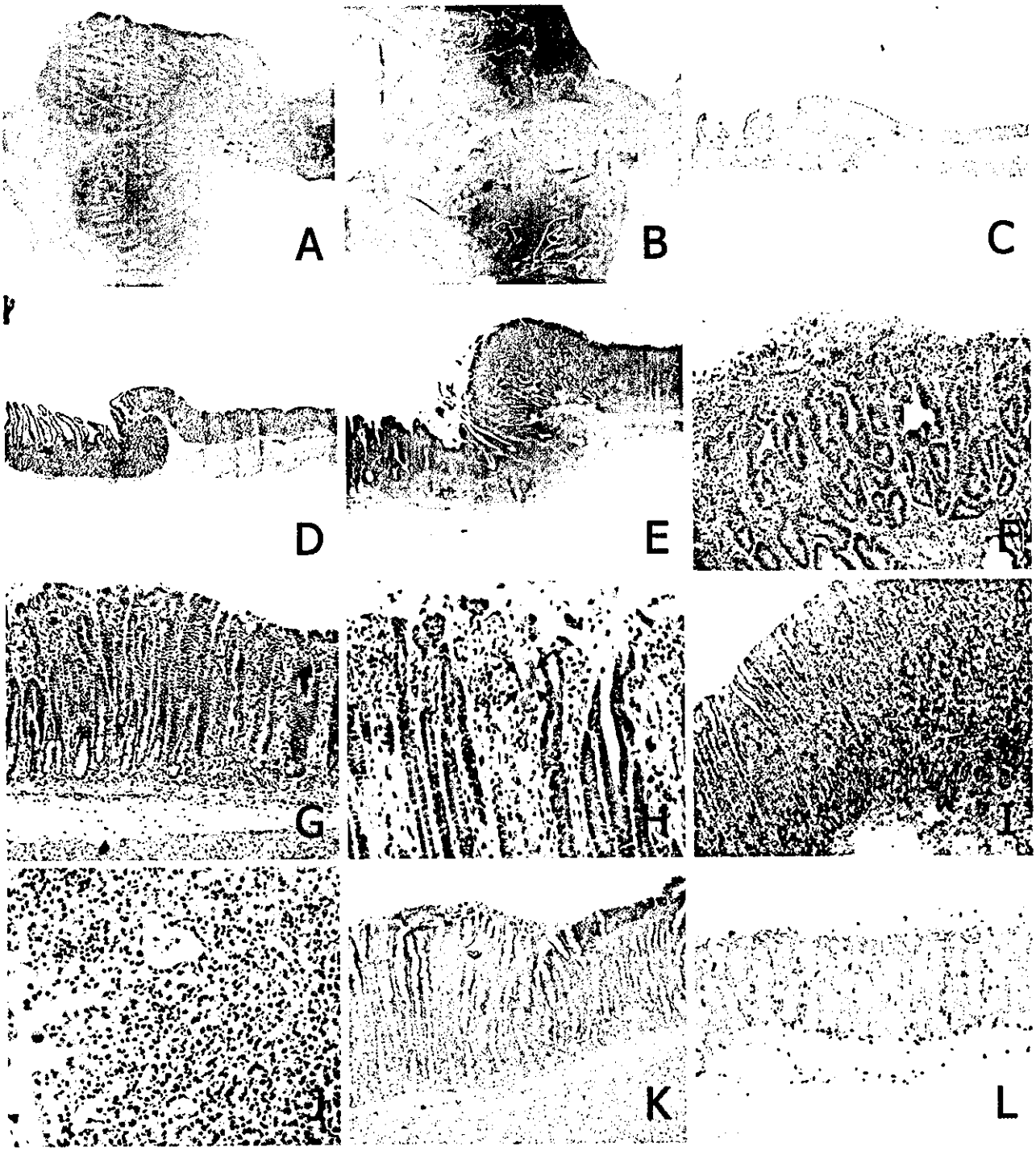

Figure 2. Macroscopic and histological features of murine gastritis. **A:** Normal stomach tissue taken from naïve $TCR^{-/-}$ mice. **B:** Inflamed stomach from $TCR^{-/-}$ mice after adoptive transfer of IL-$4^{-/-}$ RB^{Hi} T cells. **C:** The gastroduodenal junction of naïve $TCR^{-/-}$ mice. **D:** The gastroduodenal junction of the SCID recipients given IL-$4^{-/-}$ RB^{Hi} T cells. **E:** The gastroduodenal junction of the $TCR^{-/-}$ recipients given IL-$4^{-/-}$ RB^{Hi} T cells. **F:** The inflamed gastroduodenal junction with erosion. **G** and **H:** Antral gastritis with surface erosion and elongation of pits of $TCR^{-/-}$ recipients of IL-$4^{-/-}$ RB^{Hi} T cells. **Arrows** indicate a multinuclear giant cell. **I:** The fundic lesion with mild changes was taken from the same specimen as shown in **G**. **J:** Cell infiltration and dilated pits including migrating cells in the surface of the gastric fundic region in $TCR^{-/-}$ recipients of IL-$4^{-/-}$ RB^{Hi} T cells. **K:** Histochemistry for peroxidase of the antral region $TCR^{-/-}$ recipients of IL-$4^{-/-}$ RB^{Hi} T cells. As positive control, a section from a mouse with colitis induced by dextran sulfate with neutrophil infiltration was used (**L**). Sections were counterstained with methylgreen. Images were captured using a ×4 objective lens (**C**, **D** and **E**), ×20 lens (**G**, **I**, **K**, and **L**) or ×40 lens (**F**, **H**, and **J**).

thickness and exhibited an overall turbid appearance. In five recipients of IL-$4^{-/-}$ RB^{Hi} T cells, the gastric fundic area was also edematous, and erosions with petechiae were seen (Figure 2, A and B). Histological examination revealed that the inflammation was accompanied by hypertrophy of glands and elongation of pits, and these changes were most evident at the gastro-duodenal junction (Figure 2, C to F). Most typically, the antral glands were elongated more than twofold longer than their normal length with pit dilatation in some parts, and mononuclear cell infiltration in the

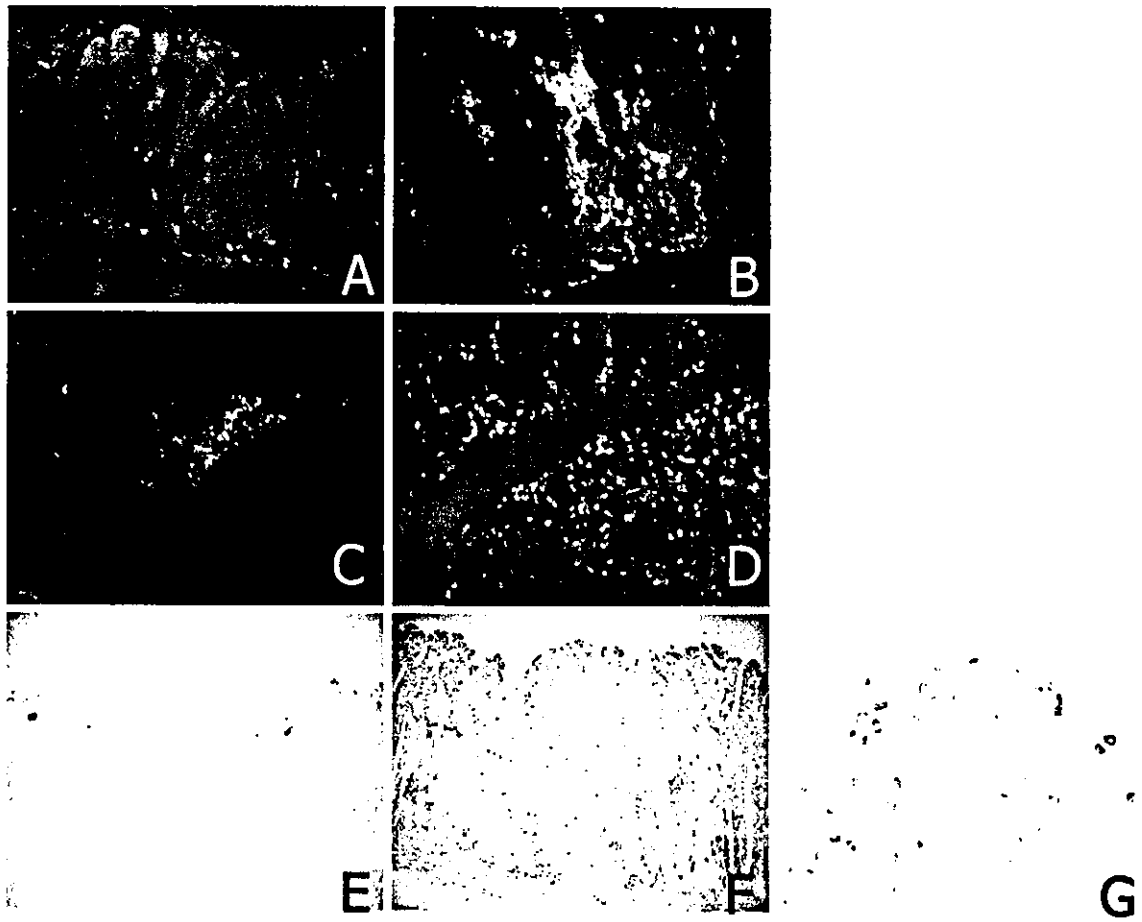

Figure 3. Immunohistochemistry and detection of apoptosis. $CD4^+$ T cells in the antrum of a SCID recipient of IL-$4^{-/-}$ RB^{Hi} T cells (**A**). $CD4^+$ T cells (**B**), $B220^+$ cells (**C**), and $CD11b^+$ cells (**D**) in the inflamed antrum of $TCR^{-/-}$ mouse recipients of IL-$4^{-/-}$ RB^{Hi} T cells. Apoptotic cells were detected by TUNEL in $TCR^{-/-}$ recipients of wt RB^{Hi} T cells (**E**) or IL-$4^{-/-}$ RB^{Hi} T cells (**F** and **G**). Images were captured using a ×20 objective lens (**A-F**) or ×100 lens (**G**).

recipients of wt and IL-$4^{-/-}$ RB^{Hi} T cells was seen (Figure 2G). In addition to these findings, recipients of IL-$4^{-/-}$ RB^{Hi} T cells developed surface erosions with multinuclear giant cell infiltration (Figure 2H). Neutrophil infiltration was not frequent in the stomach or the duodenum as shown in the histochemical reaction of myeloperoxidase (Figure 2, K and L). In 50% of IL-$4^{-/-}$ T cell recipients, a fundic inflammation with mononuclear cell infiltration and deformity of glandular pits with cells migrating into the dilated pits were seen (Figure 2J), while the other 50% of mice showed only mild changes (Figure 2I). In both cases, destruction specific for parietal cells was not seen. In the inflamed stomach, a massive infiltration of $CD4^+$ T cells occurred (Figure 3B), an event scarcely seen in SCID recipients (Figure 3A). Furthermore, B cell aggregates were also detected by staining with anti-B220 mAb (Figure 3C). We also assessed the presence of plasma cells in the inflamed areas; however, no IgG-, IgA- or IgM-containing cells were seen in the gastric mucosa by immunostaining (data not shown). The infiltrating cells were mostly macrophage-like cells as shown by staining with anti-CD11b Ab (Figure 3D). On the other hand, there was no expansion of $CD11c^+$ dendritic cells in the inflamed stomach (data not shown). Since surface erosion was enhanced in the gastric mucosa of recipients of IL-$4^{-/-}$ RB^{Hi} T cells, we also assessed apoptosis. In recipients of wt RB^{Hi} T cells, although there was elongation of glands and a cell infiltration, apoptotic cells were rare in the epithelium (Figure 3E). In contrast, in recipients of IL-$4^{-/-}$ RB^{Hi} T cells, the numbers of apoptotic cells were clearly increased. Apoptosis was readily detected in the infiltrating cells in all layers of the mucosa and especially in the surface epithelium (Figure 3, F and G).

Pathological Features of Duodenitis

Duodenal inflammation was seen in $TCR^{-/-}$ mouse recipients of both wt and IL-$4^{-/-}$ RB^{Hi} T cells. The villi and crypts were both remarkably elongated, and the villi were dilated due to the cell infiltration (Figure 4, B and C). In the lamina propria, multinuclear giant cells were frequently seen; however, granulomas were absent (Figure 4D). Immunohistological analysis revealed an infiltration of $CD4^+$ cells (Figure 4E), expansion of dendritic cells and an infiltration of macrophages (Figure 4F), which were not seen in naive $TCR^{-/-}$ mice.

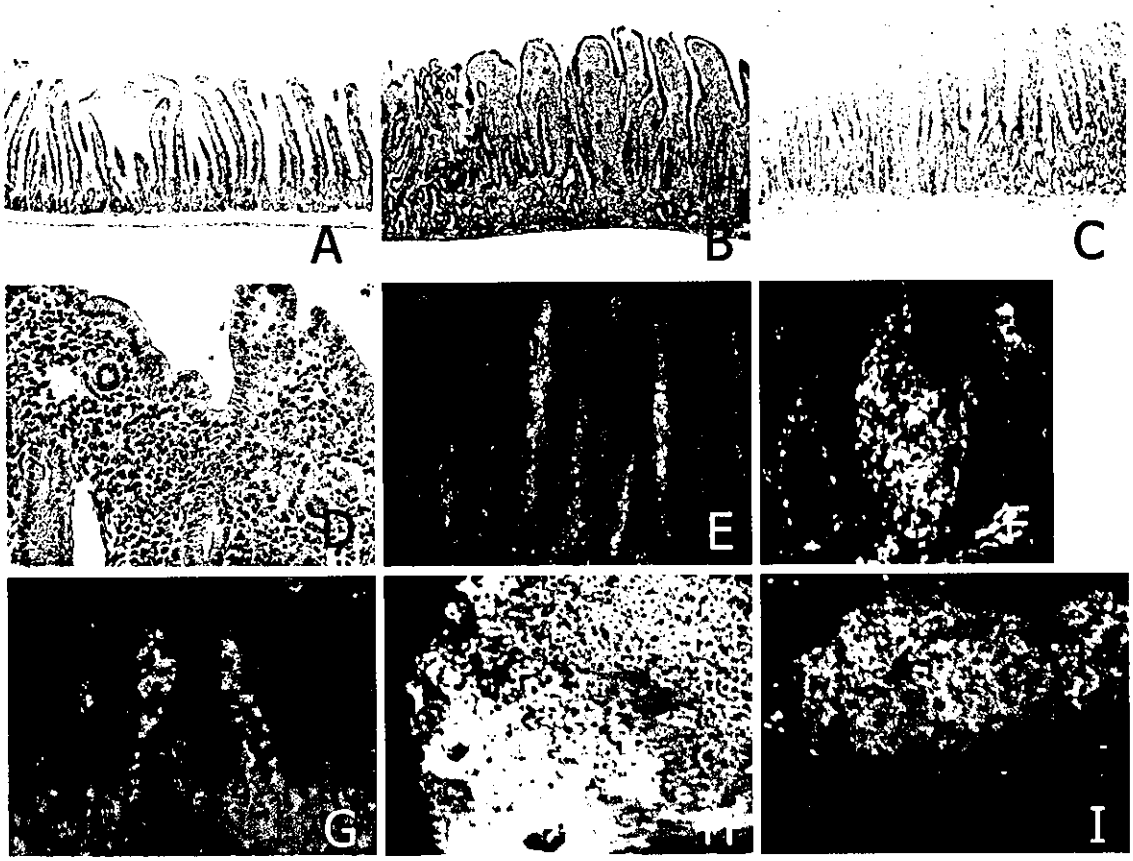

Figure 4. Histological features of murine duodenitis. **A:** H&E staining of duodenum of $TCR^{-/-}$ mice without cell transfer. **B:** Inflamed duodenum of $TCR^{-/-}$ recipients of wt RB^{Hi} T cells. **C** and **D:** Inflamed duodenum of $TCR^{-/-}$ recipients of IL-$4^{-/-}$ RB^{Hi} T cells. Dilated villus of duodenal tissue was stained with anti-CD4 (green, **E**), and anti-CD11b (green) and anti-CD11c (red) mAbs (**F**). Some $CD11c^+$ cells also express CD11b. **G:** IgA AFCs in the duodenum of recipients of wt RB^{Hi} T cells. **H:** Peyer's patches from recipients of wt RB^{Hi} T cells stained with anti-B220 (green) and anti-CD3 (red) mAbs. **I:** Peyer's patches of $TCR^{-/-}$ mice without T cell transfer. Images were captured using a ×10 objective lens (**A-C**), ×20 (**E**), or ×40 lens (**D**, **F–I**)

Production of Cytokines

To assess cytokine production by T cells that infiltrated the mucosa of adoptive hosts, $CD4^+$ T cells were isolated from LPLs of the small intestine. The $CD4^+$ T cells recovered from recipients of wt or IL-$4^{-/-}$ RB^{Hi} T cells released both IFN-γ and IL-2 (Figure 5A). It should be noted that T cells from the recipients of wt RB^{Hi} T cells also produced high levels of IL-4 (Figure 5A). We also noted that T cells infiltrating the gastric mucosa produced IFN-γ in the $TCR^{-/-}$ recipients of IL-$4^{-/-}$ T cells (Figure 5B), although T cells from recipients of IL-$4^{-/-}$ T cells tended to contain slightly more IFN-γ producing cells than recipients of wt RB^{Hi} T cells, as determined by flow cytometry (Figure 5B). Thus, IFN-γ release by T cells recovered from recipients of wt or IL-$4^{-/-}$ RB^{Hi} T cells were, for the most part, comparable. However, the lack of IL-4 secretion resulted in a remarkable phenotype, which contributed to the distinct and severe gastritis in $TCR^{-/-}$ recipients of IL-$4^{-/-}$ RB^{Hi} T cells. Further, to prove that the milder gastritis in SCID than in $TCR^{-/-}$ recipients of IL-$4^{-/-}$ RB^{Hi} T cells, we quantitatively assessed TNF-α, IFN-γ, and IL-10 by RT-PCR from total RNA extracts taken from the gastric antrum. Expression of IFN-γ and TNF-α in $TCR^{-/-}$ recipients was higher than those seen in SCID recipients (Figure 5C).

Mucosal and Systemic B Cell Responses in $TCR^{-/-}$ Recipients of RB^{Hi} T Cells

It should be noted that $TCR^{-/-}$ recipients of either wt or IL-$4^{-/-}$ RB^{Hi} T cells exhibited IgA-positive cells in the small intestine, including the duodenum (Figure 4G). Peyer's patches were also reconstituted with distinct T and B cell zones (Figure 3H), which were filled with $B220^+$ cells in $TCR^{-/-}$ mice before T cell transfer (Figure 3I). The plasma Ig levels were also elevated following adoptive transfer of either wt or IL-$4^{-/-}$ RB^{Hi} T cells. The IgG levels were comparable in both groups; however, the IgA levels were lower in recipients of IL-$4^{-/-}$ RB^{Hi} T cells than recipients of wt RB^{Hi} T cells (Figure 6A). The numbers of AFCs in the small intestine in $TCR^{-/-}$ recipients were also reconstituted by adoptive transfer of RB^{Hi} T cells. Numbers of IgG and IgA secreting cells were much less frequent in $TCR^{-/-}$ recipients of IL-$4^{-/-}$ T cells than those mice given wt T cells (Figure 6B). Thus, systemic IgG responses were fully reconstituted in both groups of mice; however, recipients of IL-$4^{-/-}$ T cells exhibited little class switching to the IgG or IgA isotypes. Plasma from these mice did not contain autoreactive Abs when assessed by the binding capacity to sections prepared from the stomach of naïve mice.

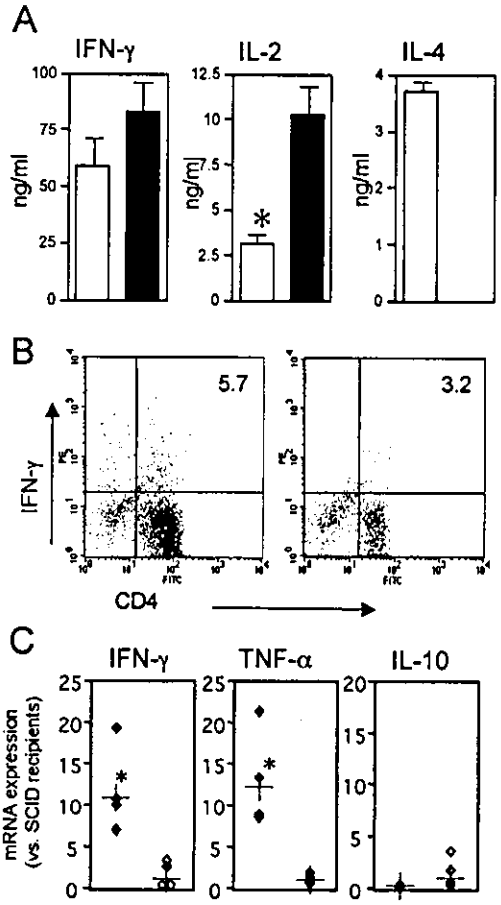

Figure 5. Production of cytokines by $CD4^+$ T cells infiltrating the GI tract. **A:** $CD4^+$ T cells were isolated from the small intestine of $TCR^{-/-}$ recipients of wt (**blank column**) or IL-$4^{-/-}$ (**solid column**) RB^{Hi} T cells and stimulated with anti-CD3 mAb for 48 hours. Culture supernatants were subjected to a cytokine ELISA. Values shown are the mean of three experiments obtained from pooled cells from three mice in each group. The results shown are the mean and SD. The difference was statistically significant. **B:** Production of IFN-γ by infiltrating cells. LPLs were prepared from the inflamed gastric mucosa of $TCR^{-/-}$ recipients of IL-$4^{-/-}$ (**left**) or wt (**right**) RB^{Hi} T cells, stimulated with anti-CD3 and anti-CD28 mAbs for 48 hours, and subjected to intracellular cytokine analysis. **C:** Relative expression of mRNA for cytokines in the stomach in $TCR^{-/-}$ and SCID recipients of IL-$4^{-/-}$ RB^{Hi} T cells determined by quantitative RT-PCR. Total RNA was extracted from the antral mucosa, and mRNA for individual cytokines and GAPDH were analyzed. Based on the average ΔC_T value of four SCID recipients, data from individual mice were shown as relative expression to SCID mice. Results from four mice are shown and the results indicated as (+) are the average of relative expression for each group. *, Statistically significant difference from SCID recipients.

Gastritis Was Dependent on the Presence of a Microflora

To this point, we found that gastritis was induced in the $TCR^{-/-}$ recipients of RB^{Hi} T cells without infection of pathogenic bacterial strains. However, the indigenous microflora in the upper GI tract or bacteria in ingested food may play a role in the induction of gastritis. To clarify this, we gave mice neomycin, streptomycin, bacitracin, and metronidazole in their drinking water following transfer of IL4$^{-/-}$ RB^{Hi} T cells. This treatment essentially eliminated the indigenous flora in the oral cavity and the stomach (Table 1), and efficiently suppressed the gastritis. Interestingly, the effect on gastritis was efficient but

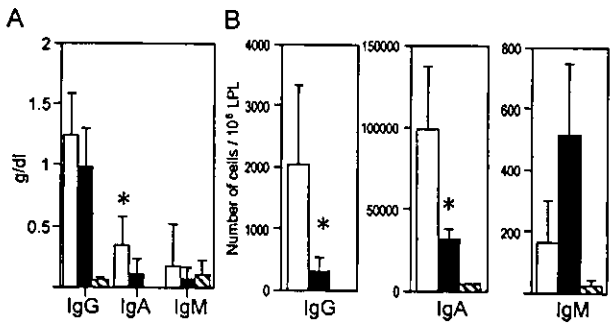

Figure 6. Reconstitution of systemic and mucosal Ig production. **A:** Plasma Ig levels in $TCR^{-/-}$ recipients of wt RB^{Hi} T cells (**blank column**), IL-$4^{-/-}$ RB^{Hi} T cells (**solid column**) or naïve $TCR^{-/-}$ mice (**shaded column**). **B:** Numbers of IgG, IgA, or IgM secreting cells in the small intestinal LPLs isolated from $TCR^{-/-}$ recipients of wt (**blank column**), IL-$4^{-/-}$ RB^{Hi} (**solid column**) or naïve $TCR^{-/-}$ mice (**hatched column**) was determined by ELISPOT assay. Values shown are the mean and a SD of each group containing 4 to 7 mice.

only partial, whereas colitis was completely blocked in these mice (Figure 7). These results indicated that induction of gastritis was partially dependent on the indigenous microflora, while colitis essentially required its presence.

Discussion

We have established a new model for gastritis that is induced by adoptive transfer of RB^{Hi} T cells incapable of production of IL-4 (Th1-prone T cells). The gastritis and duodenitis develops in the absence of a particular bacterial pathogen, such as *Helicobacter spp.* and is also distinct from autoimmune models of gastritis. The first major finding was that this pathogen-free gastritis developed after adoptive transfer of IL-$4^{-/-}$ RB^{Hi} T cells into $TCR^{-/-}$ mice. Gastritis did not occur after transfer of IL-$4^{-/-}$ RB^{Hi} T cells into SCID mice, clearly suggesting a requirement for B cell responses for full-blown gastric inflammation. Finally, adoptive transfer of IL-$4^{-/-}$ RB^{Hi} T cells yielded greater mucosal damage when compared with $TCR^{-/-}$ recipients of wt RB^{Hi} T cells. Each of these significant new findings is discussed in more detail below.

Numerous studies have attempted to establish *in vivo* models for gastric inflammation following infection with *H. pylori*. In our model, we successfully induced gastritis without bacterial infection or specific immunization. Of course, several models for autoimmune gastritis are induced in the absence of pathogens. Autoimmune disease induced by thymectomy[36,37] or ionizing radiation[38] have both resulted in gastritis. These types of gastritis were associated with damage of parietal cells or loss of parietal and chief cells by autoantibodies to the gastric H^+/K^+-ATPase.[47,48] A similar type of autoimmune gastritis occurs spontaneously in C3H/He mice.[49] "Autoimmune gastritis" and "colitis induced in SCID/Rag2$^{-/-}$ recipients of RB^{Hi} T cell transfer" are both caused by the absence of $CD4^+CD25^+$ regulatory T cells, because gastritis was induced in nu/nu mice recipients of $CD25^-$ T cells prepared from $CD25^+$ cell-depleted mice.[50] However, these two models have not been compared with each other very often. Importantly, autoimmune gastritis

Table 1. Total Viable Aerobic and Anaerobic Counts of the Whole Stomach and the Oral Mucosa of Antibiotic-Treated and Nontreated $TCR^{-/-}$ Mice (or mean CFU ± SD of 3 mice)

	Untreated	Treated
Aerobes		
Stomach (10^3 CFU/a whole stomach)		
Brain-heart infusion agar	159.3 ± 67.2	1.1 ± 0.7
Chocolate agar	167.0 ± 98.7	1.0 ± 0.6
Blood agar	80.3 ± 25.5	1.0 ± 0.5
Oral mucosa (CFU/swab)		
Brain-heart infusion agar	1969 ± 309	35 ± 36
Anaerobes		
Stomach (10^3 CFU/a whole stomach)	305.6 ± 119.7	1.2 ± 0.4
Oral mucosa (CFU/swab)	1444 ± 287	39 ± 30

induced by neonatal thymectomy was not dependent on a microflora.[51] Autoimmune gastritis was seen in germ-free mice with similar severity of inflammation, and autoantibody levels were comparable to those seen in conventional mice. In contrast, as shown in Figure 7, our gastritis model was dependent, in a significant way, on the microflora. Further, no anti-parietal cell autoantibody could be detected. Besides a requirement for a microflora and the absence of autoantibody, our model is different from autoimmune gastritis in several important ways. For example, although neonatal thymectomy caused gastritis as well as autoimmune oophoritis, orchitis, thyroiditis, pancreatitis, and prostatitis,[37,52] colitis has not been described previously. In contrast, the colon was a major organ affected by RB^{Hi} T cell transfer in SCID/$RAG2^{-/-}$/$TCR^{-/-}$ recipients, which requires the presence of a microflora. Further, in autoimmune gastritis, lesions are limited to the gastric corpus, and parietal cell destruction was the main histological feature. On the other hand, our model showed more severe inflammatory changes in the antral mucosa. Since other autoimmune disease models such as spontaneous gastritis in MRL-lpr mice were also independent of a microflora or infection,[37,52] it seems that different subsets of T regulatory cells are affected in autoimmune models and RB^{Hi} T cell-induced colitis/gastritis models. Thus, our model is quite distinct from autoimmune gastritis reported previously.

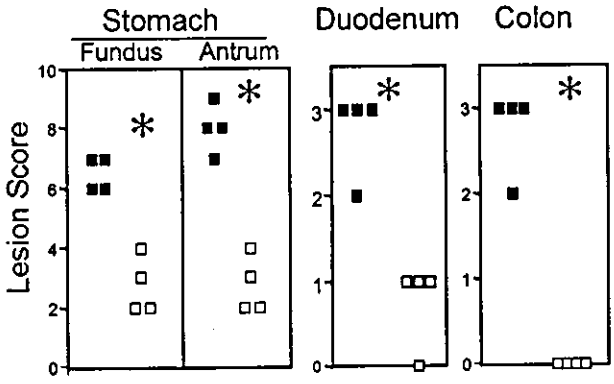

Figure 7. Treatment of recipient mice with antibiotics. A preparation of $IL\text{-}4^{-/-}$ RB^{Hi} T cells was transferred to eight $TCR^{-/-}$ mice (including two sets of male littermates in each experimental group). Four of these mice were given a combination of antibiotics in their drinking water (**blank squares**), and after 10 weeks histological scores were compared with control mice without treatment (**solid squares**).

$TCR^{-/-}$ recipients of wt or $IL\text{-}4^{-/-}$ T cells developed gastroduodenitis as well as colitis; however, no obvious changes in the jejunum or ileum were seen. This anatomical localization suggests the possible involvement of lumenal foreign antigens in the development of this type of inflammation. Colitis induced in SCID or $RAG2^{-/-}$ mice by adoptive transfer of RB^{Hi} T cells does not occur in the absence of an indigenous flora.[10,11] Through extensive testing for *Helicobacter spp.*, no pathogenic strains (including *Helicobacter* spp.) were detected in mice, which developed gastritis and duodenitis. In addition, neutrophil infiltration, which generally indicates bacterial infection, was not seen in the stomach or the duodenum in our model. On the other hand, $TCR^{-/-}$ recipients of $IL\text{-}4^{-/-}$ RB^{Hi} T cells developed a milder form of gastritis when they were treated with antibiotics. Of note, colitis was totally blocked in this group of mice. These results indicate that gastritis was partially dependent on an indigenous microflora, while colitis essentially required its presence. We speculate that orally ingested microbes or indigenous microflora in upper GI tract, in addition to food antigens, which have not been fully degradated in the stomach or duodenum, may play a similar role in this type of inflammation.

Another novel aspect of our model is the use of $TCR^{-/-}$ mice, as opposed to SCID or $RAG^{-/-}$ mice. Thus, $TCR^{-/-}$ mice lack T cells but have a fully responsive B cell repertoire. Indeed, after adoptive transfer of RB^{Hi} T cells, $TCR^{-/-}$ mice exhibit increased plasma IgG levels, and AFCs were seen in the mucosal tissues. The fact that transfer of RB^{Hi} T cells resulted in colitis and duodenitis but not gastritis in SCID mice clearly suggests the involvement of B cells in the pathogenesis of gastritis. In this regard, a different colitis model has also shown that B cells play protective roles from inflammation.[53] However, no AFCs were seen in the inflamed stomach tissues themselves, although small B cell aggregates were detected. Further, mucosal IgA production and IgA AFCs were actually lower in $TCR^{-/-}$ recipients of $IL\text{-}4^{-/-}$ RB^{Hi} T cells when compared with recipients of wt RB^{Hi} T cells, despite the more significant gastritis which characterize $IL\text{-}4^{-/-}$ RB^{Hi} T cell recipients. On the other hand, plasma IgG levels in $IL\text{-}4^{-/-}$ RB^{Hi} T cell recipients were comparable to recipients of wt RB^{Hi} T cells. The role of B cells and Ab production in our model certainly needs to be further investigated. We speculate that the presence of B cells and antibody production increases the sensitivity of

T cells to be triggered into an inflammatory expansion as well as the activation of macrophage-type cells. Our results suggest that $TCR^{-/-}$ recipients were more sensitive than SCID recipients and the former mice would be able to fully respond to the foreign antigens in the upper GI tract. To increase this sensitivity, T/B cell interactions are likely involved, although this interaction may not necessarily occur in the local mucosa but could occur in any lymphoid tissue, such as spleen or mesenteric lymph nodes. In the case of *H. pylori* infection, it is known that the presence of anti-*H. pylori* Abs are not required for the exclusion of bacteria,[53] but rather the Abs are actually involved in the pathogenesis of gastritis in humans[54] and mice due to antigenic mimicry.[55] Although we could not detect autoantibodies against the gastric parietal cells or H^+/K^+-ATPase, the presence of elevated Ig levels of particular idiotypes could play a role in the gastritis. In this regard, for our model of gastritis in the absence of infection or immunization, one could implicate molecular mimicry between any bacterial LPS and host blood group determinants[56–59] as an attractive hypothesis, although there is no direct evidence that this phenomenon actually occurs.

There is now clear evidence for a central role of T cell-mediated immunity in gastric inflammation. In the RB^{Hi} T cell transfer model described here, Th1-type cytokine production was required for the induction of colitis and gastroduodenitis, since transfer of IFN-$\gamma^{-/-}$ RB^{Hi} T cells resulted in much milder gastroduodenal inflammation (Figure 1) and colitis.[17] On the other hand, it is well known that IL-4 suppresses cytokine gene expression induced by IFN-γ and IL-2 in murine peritoneal macrophages.[60,61] The severe tissue damage in recipients of IL-$4^{-/-}$ RB^{Hi} T cells was likely caused by enhanced IFN-γ and IL-2 production by IL-$4^{-/-}$ T cells due to their predisposition toward a Th1-phenotype. However, the levels of IFN-γ release by isolated T cells were comparable in these mice. These quantitative differences in Th1 cytokines may not fully explain the fact that the epithelial cell apoptosis and surface erosion was much more frequent in IL-$4^{-/-}$ than in wt RB^{Hi} T cell recipients. Since IL-4 is a cytokine that has pleiotropic effects on a variety of cell types, including epithelial cells and other non-hematopoietic cells, a lack of IL-4 production by infiltrating T cells may have an impact on tissue repair in addition to a cytokine imbalance. Gastritis induced by infection with pathogenic *H. pylori* in IL-$4^{-/-}$ mice was more severe than that in IFN-$\gamma^{-/-}$ mice.[62] In a rat acute gastric ulcer model, healing was accompanied by a rapid rise in tissue IL-4 levels.[63] IL-$4^{-/-}$ mice were more susceptible to the colitis induced by administration of trinitrobenzene sulfonic acid, and tended to develop focal but penetrating ulcers, which were not frequently seen in IFN-$\gamma^{-/-}$ mice.[64] It is also known that fibroblasts express the IL-4 receptor, and Th2-type cells activate lung fibroblasts with resultant increase in deposition of collagen and fibronectin.[65,66] In the airway or ileal epithelium, IL-4 induces mucin gene expression[67] and goblet cell metaplasia.[17,67] Thus, IL-4 may be significantly involved in the epithelial cell turnover and tissue protection required for the maintenance of the gastrointestinal tract architecture, in addition to its role as a mediator for allowing immunological homeostasis in the gut.

In summary, we have established a novel murine model for the upper gastrointestinal tract, which does not require pathogen infection or deliberate immunization. The inflammation was mediated by Th1-type immune responses restricted to a particular subset of T cells isolated from normal mice. This model also points to the significance of the host immune system in gastric lesions and should be of importance to help better understand the pathophysiology of chronic gastroduodenitis seen in *H. pylori* infection of humans.

Acknowledgments

We thank Dr. Teruo Kirikae, Research Institute, International Medical Center of Japan, for his expert advice for bacterial culture.

References

1. Mizoguchi A, Mizoguchi E, Chiba C, Spiekermann GM, Tonegawa S, Nagler-Anderson C, Bhan AK: Cytokine imbalance and autoantibody production in T cell receptor-α mutant mice with inflammatory bowel disease. J Exp Med 1996, 183:847–856
2. Mizoguchi A, Mizoguchi E, Tonegawa S, Bhan AK: Alteration of a polyclonal to an oligoclonal immune response to cecal aerobic bacterial antigens in TCRα mutant mice with inflammatory bowel disease. Int Immunol 1996, 8:1387–1394
3. Mombaerts P, Mizoguchi E, Grusby MJ, Glimcher LH, Bhan AK, Tonegawa S: Spontaneous development of inflammatory bowel disease in T cell receptor mutant mice. Cell 1993, 75:274–282
4. Morrissey PJ, Charrier K, Braddy S, Liggitt D, Watson JD: $CD4^+$ T cells that express high levels of CD45RB induce wasting disease when transferred into congenic severe combined immunodeficient mice: disease development is prevented by cotransfer of purified $CD4^+$ T cells. J Exp Med 1993, 178:237–244
5. Powrie F, Leach MW, Mauze S, Caddle LB, Coffman RL: Phenotypically distinct subsets of $CD4^+$ T cells induce or protect from chronic intestinal inflammation in C. B-17 scid mice. Int Immunol 1993, 5:1461–1471
6. Leach MW, Bean AG, Mauze S, Coffman RL, Powrie F: Inflammatory bowel disease in C.B-17 scid mice reconstituted with the $CD45RB^{high}$ subset of $CD4^+$ T cells. Am J Pathol 1996, 148:1503–1515
7. Corazza N, Eichenberger S, Eugster HP, Mueller C: Nonlymphocyte-derived tumor necrosis factor is required for induction of colitis in recombination activating gene $(RAG)2^{-/-}$ mice upon transfer of $CD4^+CD45RB^{Hi}$ T cells. J Exp Med 1999, 190:1479–1492
8. De Jong YP, Comiskey M, Kalled SL, Mizoguchi E, Flavell RA, Bhan AK, Terhorst C: Chronic murine colitis is dependent on the CD154/CD40 pathway and can be attenuated by anti-CD154 administration. Gastroenterology 2000, 119:715–723
9. Powrie F, Leach MW, Mauze S, Menon S, Caddle LB, Coffman RL: Inhibition of Th1 responses prevents inflammatory bowel disease in SCID mice reconstituted with $CD45RB^{hi}$ $CD4^+$ T cells. Immunity 1994, 1:553–562
10. Powrie F, Mauze S, Coffman RL: CD4+ T-cells in the regulation of inflammatory responses in the intestine. Res Immunol 1997, 148:576–581
11. Aranda R, Sydora BC, McAllister PL, Binder SW, Yang HY, Targan SR, Kronenberg M: Analysis of intestinal lymphocytes in mouse colitis mediated by transfer of $CD4^+$, $CD45RB^{high}$ T cells to SCID recipients. J Immunol 1997, 158:3464–3473
12. Powrie F, Carlino J, Leach MW, Mauze S, Coffman RL: A critical role for transforming growth factor-β but not interleukin 4 in the suppression of T helper type 1-mediated colitis by $CD45RB^{low}$ $CD4^+$ T cells. J Exp Med 1996, 183:2669–2674
13. Asseman C, Mauze S, Leach MW, Coffman RL, Powrie F: An essential

role for interleukin 10 in the function of regulatory T cells that inhibit intestinal inflammation. J Exp Med 1999, 190:995–1004
14. Read S, Malmstrom V, Powrie F: Cytotoxic T lymphocyte-associated antigen 4 plays an essential role in the function of $CD25^+CD4^+$ regulatory cells that control intestinal inflammation. J Exp Med 2000, 192:295–302
15. McGhee JR, Kiyono H: Mucosal immunology. Fundamental Immunology. Edited by Paul WE. San Diego, Academic Press, 1999, pp 909–945
16. McGhee JR, Lamm ME, Strober W: Mucosal immune responses: an overview. Mucosal Immunology. Edited by Ogra P. San Diego, Academic Press, 1999, pp 485–506
17. Dohi T, Fujihashi K, Koga T, Shirai Y, Kawamura YI, Ejima C, Kato R, Saitoh K, McGhee JR: T helper type-2 cells induce ileal villus atrophy, goblet cell metaplasia, and wasting disease in T cell-deficient mice. Gastroenterology 2003, 124:672–682
18. Blum AL: Treatment of acid-related disorders with gastric acid inhibitors: the state of the art. Digestion 1990, 47(Suppl 1):3–10
19. Czinn SJ, Blaser MJ, Nedrud JG: Peptic ulcers and gastritis. Mucosal Immunology. Edited by Ogra P. San Diego, Academic Press, 1999, pp 1035–1046
20. Marshall BJ, Armstrong JA, McGecie DB: Attempt to fulfill Koch's postulates for pyloric Campylobacter. Med J Aust 1985, 142:436–439
21. Fox JG, Lee A: The role of Helicobacter species in newly recognized gastrointestinal tract diseases of animals. Lab Anim Sci 1997, 47: 222–255
22. Eaton KA, Radin MJ, Krakowka S: An animal model of gastric ulcer due to bacterial gastritis in mice. Vet Pathol 1995, 32:489–497
23. Czinn SJ, Cai A, Nedrud JG: Oral immunization protects germ-free mice against infection from Helicobacter felis. Gastroenterology 1992, 102:A611
24. Lee A, Fox JG, Otto G, Murphy J: A small animal model of human Helicobacter pylori active chronic gastritis. Gastroenterology 1990, 99:1315–1323
25. Nedrud JG, Blanchard SS, Czinn SJ: Helicobacter pylori inflammation and immunity. Helicobacter 2002, 7:24–29
26. Chen W, Shu D, Chadwick VS: Helicobacter pylori infection: mechanism of colonization and functional dyspepsia: reduced colonization of gastric mucosa by Helicobacter pylori in mice deficient in interleukin-10. J Gastroenterol Hepatol 2001, 16:377–383
27. Eaton KA, Kersulyte D, Mefford M, Danon SJ, Krakowka S, Berg DE: Role of Helicobacter pylori cag region genes in colonization and gastritis in two animal models. Infect Immun 2001, 69:2902–2908
28. Michetti P, Corthesy-Theulaz I, Davin C, Haas R, Vaney A-C, Heitz M, Bille J, Kraehenbuhl J-P, Saraga E, Blum AL: Immunization of BALB/c mice against Helicobacter felis infection with Helicobacter pylori urease. Gastroenterology 1994, 107:1002–1011
29. Pappo J, Thomas WDJ, Kabok Z, Taylor NS, Murphy JC, Fox JG: Effect of oral immunization with recombinant urease on murine Helicobacter felis gastritis. Infect Immun 1995, 63:1246–1252
30. Lee CK, Weltzin R, Thomas Jr WD, Kleanthous H, Ermak TH, Soman G, Hill JE, Ackerman SK, Monath TP: Oral immunization with recombinant Helicobacter pylori urease induces secretory IgA antibodies and protects mice from challenge with Helicobacter felis. J Infect Dis 1995, 172:161–172
31. Eaton KA, Ringler SR, Danon SJ: Murine splenocytes induce severe gastritis and delayed-type hypersensitivity and suppress bacterial colonization in Helicobacter pylori-infected SCID mice. Infect Immun 1999, 67:4594–4602
32. Tushi MF, Sorensoen RU, Czinn SJ: Cell-mediated immune responsiveness to Helicobacter pylori in healthy seropositive and seronegative adults. Immun Infect Dis 1992, 2:133–136
33. D'Elios MM, Manghetti M, De Carli M, Costa F, Baldari CT, Burroni D, Telford JL, Romagnani S, Del Prete G: T helper 1 effector cells specific for Helicobacter pylori in the gastric antrum of patients with peptic ulcer disease. J Immunol 1997, 158:962–967
34. D'Elios MM, Amedei A, Manghetti M, Costa F, Baldari CT, Quazi AS, Telford JL, Romagnani S, Del Prete G: Impaired T-cell regulation of B-cell growth in Helicobacter pylori-related gastric low-grade MALT lymphoma. Gastroenterology 1999, 117:1105–1112
35. Maloy KJ, Salaun L, Cahill R, Dougan G, Saunders NJ, Powrie F: $CD4^+CD25^+$ T(R) cells suppress innate immune pathology through cytokine-dependent mechanisms. J Exp Med 2003, 197:111–119
36. Nishizuka Y, Sakakura T: Thymus and reproduction: sex-linked dysgenesia of the gonad after neonatal thymectomy in mice. Science 1969, 166:753–755
37. Fukuma K, Sakaguchi S, Kuribayashi K, Chen WL, Morishita R, Sekita K, Uchino H, Masuda T: Immunologic and clinical studies on murine experimental autoimmune gastritis induced by neonatal thymectomy. Gastroenterology 1988, 94:274–283
38. Sakaguchi N, Miyai K, Sakaguchi S: Ionizing radiation and autoimmunity: induction of autoimmune disease in mice by high dose fractionated total lymphoid irradiation and its prevention by inoculating normal T cells. J Immunol 1994, 152:2586–2595
39. Shames B, Fox JG, Dewhirst F, Yan L, Shen Z, Taylor NS: Identification of widespread Helicobacter hepaticus infection in feces in commercial mouse colonies by culture and PCR assay. J Clin Microbiol 1995, 33:2968–2972
40. Riley LK, Franklin CL, Hook RR, Besch-Williford C: Identification of murine Helicobacters by PCR and restriction enzyme analyses. J Clin Microbiol 1996, 34:942–946
41. Goto K, Ohashi H, Takakura A, Itoh T: Current status of Helicobacter contamination of laboratory mice, rats, gerbils, and house musk shrews in Japan. Curr Microbiol 2000, 41:161–166
42. Battles JK, Williamson JC, Pike KM, Gorelick PL, Ward JM, Gonda MA: Diagnostic assay for Helicobacter hepaticus based on nucleotide sequence of its 16S rRNA gene. J Clin Microbiol 1995, 33:1344–1347
43. Dohi T, Fujihashi K, Rennert PD, Iwatani K, Kiyono H, McGhee JR: Hapten-induced colitis is associated with colonic patch hypertrophy and T helper 2-type responses. J Exp Med 1999, 189:1169–1180
44. Fujihashi K, McGhee JR, Kweon M-N, Cooper MD, Tonegawa S, Takahashi I, Hiroi T, Mestecky J, Kiyono H: γ/δ T cell-deficient mice have impaired mucosal immunoglobulin A responses. J Exp Med 1996, 183:1929–1935
45. Yoshino N, Ami Y, Terao K, Tashiro F, Honda M: Upgrading of flow cytometric analysis for absolute counts, cytokines and other antigenic molecules of cynomolgus monkeys (Macaca fascicularis) by using anti-human cross-reactive antibodies. Exp Anim 2000, 49:97–110
46. Simpson SJ, Shah S, Comiskey M, YP d, Wang B, Mizoguchi E, Bhan AK, Terhorst C: T cell-mediated pathology in two models of experimental colitis depends predominantly on the interleukin 12/signal transducer and activator of transcription (Stat)-4 pathway, but is not conditional on interferon γ expression by T cells. J Exp Med 1998, 187:1225–1234
47. Jones CM, Callaghan JM, Gleeson PA, Mori Y, Masuda T, Toh BH: The parietal cell autoantigens recognized in neonatal thymectomy-induced murine gastritis are the α and β subunits of the gastric proton pump. Gastroenterology 1991, 101:287–294
48. Toh BH, Gleeson PA, Simpson RJ, Moritz RL, Callaghan JM, Goldkorn I, Jones CM, Martinelli TM, Mu FT, Humphris DC, JM P, Mori Y, Masuda T, Sobieszczuk P, Weinstock J, Mantamadiotis T, Baldwin G: The 60- to 90-kDa parietal cell autoantigen associated with autoimmune gastritis is a β subunit of the gastric H+/K(+)-ATPase (proton pump). Proc Natl Acad Sci USA 1990, 87:6418–6422
49. Alderuccio F, Toh BH: Spontaneous autoimmune gastritis in C3H/He mice: a new mouse model for gastric autoimmunity. Am J Pathol 1998, 153:1311–1318
50. McHugh RS, Shevach EM: Cutting edge: depletion of $CD4^+CD25^+$ regulatory T cells is necessary, but not sufficient, for induction of organ-specific autoimmune disease. J Immunol 2002, 168:5979–5983
51. Murakami K, Muruyama H, Hosono M, Sinagawa K, Yamada J, Kuribayashi K, Masuda T: Germ-free condition and the susceptibility of BALB/c mice to post-thymectomy autoimmune gastritis. Autoimmunity 1992, 12:69–70
52. Maldonado MA, Kakkanaiah V, MacDonald GC, Chen F, Reap EA, Balish E, Farkas WR, Jennette JC, Madaio MP, Kotzin BL, Cohen PL, Eisenberg RA: The role of environmental antigens in the spontaneous development of autoimmunity in MRL-lpr mice. J Immunol 1999, 162:6322–6330
53. Garhart CA, Nedrud JG, Heinzel FP, Sigmund NE, Czinn SJ: Vaccine-induced protection against Helicobacter pylori in mice lacking both antibodies and interleukin-4. Infect Immun 2003, 71:3628–3633
54. Sugiyama T, Yabana T, Yachi A: Mucosal immune response to Helicobacter pylori and cytotoxic mechanism. Scand J Gastroenterol Suppl 1995, 208:30–32

55. Negrini R, Savio A, Poiesi C, Appelmelk B, Buffoli F, Paterlini A, Cesari P, Graffeo M, Vaira D, Franzin G: Antigenic mimicry between Helicobacter pylori and gastric mucosa in the pathogenesis of body atrophic gastritis. Gastroenterology 1996, 111:655–665
56. Appelmelk BJ, Simoons-Smit I, Negrini R, Moran AP, Aspinall GO, Forte JG, De Vries T, Quan H, Verboom T, Maaskant JJ, Ghiara P, Kuipers EJ, Bloemena E, Tadema TM, Townsend RR, Tyagarajan K, Crothers Jr JM, Monteiro MA, Savio A, De Graaff J: Potential role of molecular mimicry between Helicobacter pylori lipopolysaccharide and host Lewis blood group antigens in autoimmunity. Infect Immun 1996, 64:2031–2040
57. Aspinall GO, Monteiro MA: Lipopolysaccharides of Helicobacter pylori strains P466 and MO19: structures of the O antigen and core oligosaccharide regions. Biochemistry 1996, 35:2498–2504
58. Simoons-Smit IM, Appelmelk BJ, Verboom T, Negrini R, Penner JL, Aspinall GO, Moran AP, Fei SF, Shi BS, Rudnica W, Savio A, de Graaff J: Typing of Helicobacter pylori with monoclonal antibodies against Lewis antigens in lipopolysaccharide. J Clin Microbiol 1996, 34: 2196–2200
59. Wirth HP, Yang M, Karita M, Blaser MJ: Expression of the human cell surface glycoconjugates Lewis x and Lewis y by Helicobacter pylori isolates is related to cagA status. Infect Immun 1996, 64:4598–4605
60. Gautam S, Tebo JM, Hamilton TA: IL-4 suppresses cytokine gene expression induced by IFN-γ and/or IL-2 in murine peritoneal macrophages. J Immunol 1992, 148:1725–1730
61. Ohshima Y, Yang LP, Avice MN, Kurimoto M, Nakajima T, Sergerie M, Demeure CE, Sarfati M, Delespesse G: Naive human CD4$^+$ T cells are a major source of lymphotoxin α. J Immunol 1999, 162:3790–3794
62. Smythies LE, Waites KB, Lindsey JR, Harris PR, Ghiara P, Smith PD: Helicobacter pylori-induced mucosal inflammation is Th1 mediated and exacerbated in IL-4, but not IFN-γ, gene-deficient mice. J Immunol 2000, 165:1022–1029
63. Slomiany BL, Piotrowski J, Slomiany A: Down-regulation of endothelin-1 by interleukin-4 during gastric ulcer healing. Biochem Biophys Res Commun 1999, 263:591–595
64. Dohi T, Fujihashi K, Kiyono H, Elson CO, McGhee JR: Mice deficient in Th1- and Th2-type cytokines develop distinct forms of hapten-induced colitis. Gastroenterology 2000, 119:724–733
65. Derdak S, Penney DP, Keng P, Felch ME, Brown D, Phipps RP: Differential collagen and fibronectin production by Thy 1$^+$ and Thy 1$^-$ lung fibroblast subpopulations. Am J Physiol 1992, 263:L283–L290
66. Roche WR, Beasley R, Williams JH, Holgate ST: Subepithelial fibrosis in the bronchi of asthmatics. Lancet 1989, 1:520–524
67. Dabbagh K, Takeyama K, Lee HM, Ueki IF, Lausier JA, Nadel JA: IL-4 induces mucin gene expression and goblet cell metaplasia in vitro and in vivo. J Immunol 1999, 162:6233–6237

Altered expression of NDST-1 messenger RNA in puromycin aminonucleoside nephrosis

KENJI NAKAYAMA, YUMIKO NATORI, TOSHINOBU SATO, TOMOYOSHI KIMURA, AKIRA SUGIURA, HIROSHI SATO, TAKAO SAITO, SADAYOSHI ITO, and YASUHIRO NATORI

TOKYO, SENDAI, and FUKUOKA, JAPAN

Sulfated portions of glycosaminoglycan (GAG) side chains in heparan sulfate proteoglycan (HSPG) are thought to play an important role in charge-dependent selectivity of glomerular filtration against plasma proteins. Heparan sulfate *N*-acethylglucosamine *N*-deacethylase/adenosine 3'-phosphate 5'-phosphosulfate: unsubstituted glucosamine *N*-sulfotransferase (NDST) is the key enzyme regulating sulfation of GAG chains. In this study we investigated transcriptional expression of NDST-1, 1 of 4 isozymes of NDST, in glomeruli of rats with puromycin aminonucleoside (PAN) nephrosis. Nephrosis was induced in rats with a single intraperitoneal injection of 150 mg/kg PAN. On days 10 and 35, expression of NDST-1 messenger RNA (mRNA) in glomeruli was analyzed with the use of Northern-blot analysis. Immunohistochemical studies were also performed with the use of monoclonal antibodies that react specifically with the *N*-sulfated portion of the GAG chain of HSPG and agrin, a major core protein of HSPG in glomerular basement membrane (GBM). In addition, we studied the expression of NDST-1 mRNA in cultured glomerular epithelial cells (GECs) and glomerular mesangial cells in the presence of PAN. On day 10, when significant proteinuria developed, the ratios of glomerular expression of NDST-1 mRNA against glyceraldehyde-phosphate dehydrogenase mRNA in PAN-treated rats were decreased to 48% ± 6% of those in controls ($P < .05$). Immunohistochemical studies revealed that staining for *N*-sulfated GAG chains of HSPG on GBM was markedly reduced on day 10 in PAN-treated rats but that staining for agrin was unchanged. In contrast, on day 35, when PAN-treated rats recovered from proteinuria, we noted no differences in glomerular expression of NDST-1 mRNA and staining intensity for *N*-sulfated GAG chains on GBM between PAN-treated rats and controls. Incubation of GECs for 24 hours in the presence of 50 ng/mL PAN resulted in the reduction of the expression of NDST-1 mRNA (67% ± 12% of those in controls, $P < .05$). In summary, we found alteration of the expression of NDST-1 mRNA, accompanying a loss of *N*-sulfated GAG chains of HSPG on GBM without changes in the core protein agrin, in the course of PAN nephrosis. These data suggest an important role for this enzyme in heparan sulfate assembly in GBM and GEC and in the pathogenesis of proteinuria in PAN nephrosis. (J Lab Clin Med 2004; 143:106-14)

From the Research Institute, International Medical Center of Japan Tokyo,Japan; the Division of Nephrology, Endocrinology and Vascular Medicine, Department of Medicine and Department of Blood Purification, Tohoku University Hospital, Sendai, Japan; and the Fourth Department of Internal Medicine, Fukuoka University School of Medicine.

Supported in part by a grant for cardiovascular research from the Ministry of Health and Welfare of Japan (13C-5) and a grant from the Ministry of Science, Education, and Culture of Japan (15390264).

Submitted for publication October 17, 2003; revision submitted October 29, 2003; accepted October 29, 2003.

Reprints requests: Kenji Nakayama, MD, Division of Nephrology, Endocrinology, and Vascular Medicine, Department of Medicine, Tohoku University School of Medicine, 1-1 Seiryo-Cho, Aoba-Ku, Sendai 980-8574, Japan.

0022-2143/$ – see front matter

© 2004 Elsevier Inc. All rights reserved.

doi:10.1016/j.jab.2003.10.012

Abbreviations: cDNA = complementary DNA; dCTP = deoxycytidine triphosphate; DMEM = Dulbecco's modified Eagle medium; EDTA = ethylenediaminetetraacetate; FCS = fetal calf serum; GAG = glycosaminoglycan; GAPDH = glyceraldehyde-3-phosphate dehydrogenase; GBM = glomerular basement membrane; GEC = glomerular epithelial cell; GMC = glomerular mesangial cell; GlcN = unsubstituted glucosamine; GlcNAc = *N*-acetylglucosamine; HEPES = *N*-2-hydroxyethylpiperazine-*N*-2-ethanesulfonic acid; HSPG = heparan sulfate proteoglycan; kb = kilobase; mRNA = messenger RNA; NDST = heparan sulfate GlcNAc *N*-deacethylase/PAPS:GlcN *N*-sulfotransferase; PAN = puromycin aminonucleoside; PAPS = adenosine 3'-phosphate 5'-phosphosulfate; PAS = periodic acid-Schiff; PBS = phosphate-buffered saline solution; PCR = polymerase chain reaction; ROS = reactive oxygen species; SDS = sodium dodecyl sulfate; SSC = standard saline citrate

Studies in both human and experimental animals indicate that the defect of size- and charge-selective barrier of the glomerular capillary wall results in the development of proteinuria, a most important and common manifestation of glomerular diseases.[1-3] Structural gaps in endothelial fenestrae, foot processes of visceral GECs, and special composition of extracellular matrix in the GBM contribute to the size-selective barrier of glomerular capillary wall.[4] The status of anionic sites in the glomerular capillary wall determines the charge-dependent selectivity.[2,5] These anionic sites are constituted by physiological anionic molecules such as HSPG in GBM and cell-surface sialoglycoproteins.[6-8] HSPG is located most densely in lamina rara interna and externa of GBM.[9] Biochemical studies suggest that sulfated portions of GAG side chains of HSPG are responsible for anionic charge in the HSPG molecule.[10-12]

It has been shown that changes in HSPG molecules, including sulfated portions in the GAG chains, are involved in the development of proteinuria in human renal diseases and in experimental models such as PAN nephrosis.[11-16] However, few studies have investigated the process that regulates sulfation of GAG chains of HSPG in the kidney. NDST is the enzyme catalyzing *N*-sulfation of unsulfated "backbone" disaccharide chains of HSPG, and the *N*-sulfation is essential for further sulfation of GAG chains.[17,18] It is possible that the disturbance of NDST is closely related to proteinuria in certain glomerular diseases, but the involvement of NDST remains to be determined.[19]

In this study, we investigated the alteration of gene expression of NDST-1, 1 of 4 isozymes of NDST,[20,21] in glomeruli in the presence of acute PAN nephrosis, a well-known experimental model of nephrotic syndrome.[22] We also studied the in vitro effect of PAN on NDST-1 mRNA expression using cultured GECs because GECs are thought to play an important role in the synthesis of HSPG in GBM.[9,23,24]

The present data indicated that NDST-1 mRNA expression is decreased with the reduction of the *N*-sulfated portion of heparan sulfate in the nephrotic state and returns to normal in the recovery state of PAN nephrosis.

METHODS

Animals. We obtained age-matched male Wistar and Sprague-Dawley rats weighing 180 to 200 g from Charles River Japan (Atsugi, Japan) and kept them in our accredited animal facilities with free access to pelleted food (Oriental Yeast Co, Ltd., Tokyo, Japan) and tap water. Animal experiments were conducted in accordance with the guidelines set forth in the National Institutes Health *Guide for the Care and Use of Laboratory Animals* (pub no 85-23).

Materials. We purchased PAN (Sigma-Aldrich, St Louis, Mo), Dulbecco's modified Eagle medium (DMEM), DMEM/Ham's F-12 medium (Gibco Laboratories, Grand Island, NY), FCS, epidermal growth factor, ITS+ premix (Collaborative Research, Inc, Bedford, Mass), OCT compound (Miles, Inc, Elkhart, Ind), phosphorus 32–labeled dCTP (NEN Research Products, Boston, Mass), a random-primed DNA-labeling kit (Boehringer Mannheim Biochemica, Mannheim, Germany), mouse monoclonal antibody against *N*-sulfated glucosamine-enriched portion of heparan sulfate (F58-10E4)[25] (Seikagaku Corp, Tokyo, Japan), fluorescein isothiocyanate–conjugated goat anti-mouse IgG + IgM antibody and goat anti-hamster IgG antibody (Jackson ImmunoResearch, West Grove, Pa) as indicated. Hamster monoclonal antibody MI90 against rat agrin,[26] a major HSPG core protein in glomeruli,[27] was provided by Professor Jo H. M. Berden (Department of Nephrology, Nijmegen University Hospital, Nijmegen, The Netherlands).

A 2.4-kb cDNA probe specific for rat NDST-1[28] and a 1.3-kb cDNA probe specific for GAPDH[29] were prepared from the plasmids provided by Dr Carlos B. Hirschberg (Department of Biochemistry and Molecular Biology, University of Massachusetts Medical Center, Worcester, Mass) and Dr Ph. Fort (Institut de Génétique Moléculaire, Université Montpellier, Montpellier, France), respectively.

Animal model. We divided 20 Wistar rats into 2 groups of 10 rats each. In 1 group, PAN nephrosis was induced with an intraperitoneal injection of 150 mg/kg PAN dissolved in 2 mL of saline solution.[30] Rats in the other group were injected with saline solution alone and used as controls. Five rats in each group were killed under diethyl ether anesthesia on days 10 and 35. These time points were chosen because previous studies had shown that massive proteinuria developed by day 10 and disappeared by day 35 after the single 150 mg/kg

injection of PAN.[30] Immediately after animals were killed, the kidneys were processed for histological study and Northern-blot analysis as described below. The entire experiment was repeated 3 times independently.

Twenty-four-hour urine and blood samples were collected from each rat before it was killed. Urinary protein was determined as daily excretion in 24-hour urine with the use of the Biuret method as reported previously.[31] Serum concentrations of albumin, creatinine, and total cholesterol were measured with a Synchron CX3 chemical analyzer (Beckman, Tokyo, Japan) or Dri-Chem 5000 analyzer (Fuji Film, Tokyo, Japan).

Histologic studies. For light microscopy, renal tissue was fixed in 95% ethanol for 24 hours at 4°C and embedded in paraffin as described previously.[32] Two-micrometer sections were stained with PAS or periodic acid methenamine silver in accordance with conventional methods. For electron microscopy, we fixed blocks (1.5 mm^3) of renal tissue in 2.5% glutaraldehyde and 2% paraformaldehyde followed by postfixation with 1% osmium tetroxide. The blocks were then dehydrated and embedded in Epon 812 (TAAB Laboratories Equipment Ltd., Aldermaston, Berkshire, England). Ultrathin sections (60 nm) were mounted on coated copper grids, stained with uranyl acetate and lead citrate, and then examined with a JEOL 1010 electron microscope (Nippon Denshi, Tokyo, Japan).[33]

For immunohistochemistry, we embedded renal tissue in OCT compound, snap-froze it in precooled hexane, and stored it in liquid nitrogen until use. Four-micrometer cryostat sections were air-dried and fixed in acetone for 10 minutes at room temperature. *N*-sulfated portions of GAG chains in HSPG and agrin were detected with the use of a standard immunofluorescence method with monoclonal antibodies F58-10E4[25] and anti-agrin MI90,[26] respectively. In brief, the specimens were incubated with the antibodies diluted in PBS at a ratio of 1:100 for 1 hour at 37°C. After 3 washes with PBS, the specimens were further incubated with fluorescein isothiocyanate–goat anti-mouse IgG + IgM antibody or goat anti-hamster IgG antibody (Jackson) diluted in PBS at a ratio of 1:100 for 1 hour at 37°C. They were washed again with PBS, then examined under a BH2 RFL T2 fluorescence microscope (Olympus Optical Co, Ltd, Tokyo, Japan). Photographs were taken with a PM-10AD automatic timer (Olympus). Two of the authors independently examined the kidney sections and scored the intensity of staining for 10E4 and agrin in GBM of each glomerulus semiquantitatively, using an arbitrary scale of 4 grades (0–3), depending on the degree of staining intensity. The mean and SD in all groups of 5 rats were calculated, with an average score of 30 glomeruli for each rat specimen.

Cell culture. GECs isolated from Sprague-Dawley rats were provided by Dr Hideaki Yamabe (Second Department of Internal Medicine, Hirosaki University School of Medicine, Hirosaki, Japan).[34,35] GECs were cultured in plates coated with collagen type I in DMEM-H containing 5% FCS, 2 mmol/L L-glutamine, 10 ng/mL epithelial growth factor, and 1% ITS+ premix.[36] GMCs were isolated from Sprague-Dawley rats and maintained in DMEM containing 10% FCS, 2 mmol/L L-glutamine and 1% ITS+ premix as described previously.[29]

For experiments, confluent GECs were washed 3 times with DMEM-H containing 0.5% FCS and incubated with DMEM-H containing 0.5% FCS in the absence or the presence of PAN at various concentrations (5–500 ng/mL). Confluent GMCs were washed and treated in the same manner with DMEM containing 0.5% FCS. After incubation, cells were washed 3 times with PBS, frozen with liquid nitrogen, and stored at −80°C until use for RNA isolation. After incubation of GECs with PAN, cell viability was determined with the use of the trypan blue exclusion test.

RNA isolation and Northern-blot analyses. On days 10 and 35 after injection of PAN or saline solution, we isolated glomeruli from the kidneys using the sequential-sieving method.[37] The glomeruli from 5 rats in each group were pooled, and total RNA was isolated from the pooled glomeruli with the use of the acid-guanidium-phenol-chloroform method.[38] Cellular RNA was also isolated from cultured GECs and GMCs. After determining the amount of RNA with a spectrophotometer, we applied 30 μg of each RNA to 1.0% agarose gel containing 2.2 mol/L formaldehyde, subjected the gels to electrophoresis for 4 hours at 100 V and blotted them to nitrocellulose membrane. Prehybridization and hybridization were performed in a solution containing 50% formaldehyde, 50 mmol/L HEPES-KOH (pH 7.3), 1 mmol/L EDTA, 0.2% SDS, 3× SSC, and 5× Denhart's solution. After 2 hours of prehybridization at 42°C with 200 μg/mL of denatured salmon-sperm DNA, hybridization was performed at 42°C overnight with cDNA for rat NDST-1 radiolabeled with [32P]dCTP. After hybridization, the blot was washed extensively with 1× SSC–0.1% SDS at 42°C for 20 minutes and then 1× SSC - 0.1% SDS at 68°C three times for 20 minutes each. Control hybridization was performed with cDNA for rat GAPDH. Autoradiography to detect NDST-1 mRNA and GAPDH mRNA, respectively, was performed for 24 or 6 hours at room temperature with a BAS Imaging Plate (Fuji Film). Expression of each mRNA was measured quantitatively with the BAS-2000 system (Fuji Film), and the expression of NDST-1 mRNA was calculated as a relative ratio against that of GAPDH mRNA. The results were expressed as a percentage of the ratio relative to those in control.

Real-time PCR. For the quantitative measurement of NDST-1 mRNA levels in GMC, we performed real-time polymerase chain reaction using the ABI PRISM 7700 Sequence Detector and TaqMan Predeveloped Assay Reagents for the Gene Expression Quantification System (Applied Biosystems, Foster City, Calif). Using multiple reporter dyes, we assayed the mRNA levels of NDST-1 and endogenous control (GAPDH). NDST-1 mRNA levels were expressed as the ratio relative to the endogenous control. The sequence of the probes were as follows: forward primer sequence, ACTCATATTGAACGCTGGCTCA; reverse primer sequence, TCTGCACTGTGTCCATCACTTTG; TaqMan probe sequence, CATGCCAACCAGATCCTGGTCTTGGAT.

Statistical analysis. All values are expressed as mean ± SD. Data were analyzed with the use of Student's *t* test for unpaired samples or the Spearman rank-correlation coefficient. *P* values of less than .05 were considered statistically significant.

Table I. Summary of blood and urine analyses

Treatment group	Urinary protein (mg/day)	Albumin (g/dL)	Cholesterol (mg/dL)	Creatinine (mg/dL)
PAN				
Day 10	853.9 ± 152.0*	0.78 ± 0.13*	353.3 ± 20.0*	0.35 ± 0.06
Day 35	53.0 ± 32.7	3.55 ± 0.13	95.0 ± 2.7	0.33 ± 0.05
Saline solution				
day 10	21.6 ± 2.2	3.02 ± 0.08	115.2 ± 5.5	0.36 ± 0.05
day 35	27.7 ± 12.3	3.45 ± 0.13	82.8 ± 4.7	0.43 ± 0.05

Data expressed as the mean ± SD (n = 5).
*$P < .05$ vs controls at each time point.

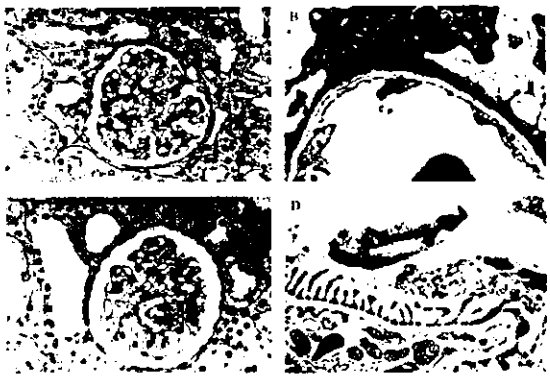

Fig 1. Representative photographs of renal histology under light microscopy (*A* and *C*, PAS staining, original magnification 200×) and electron microscopy (*B* and *D*, original magnification 16,000×). On day 10 after injection of PAN we detected no apparent changes under light microscopy (A) and effacement of foot processes of GECs under electron microscopy (B). We noted no abnormalities in histology on day 35 in PAN-treated rats (C and D).

RESULTS

Clinical and histological analyses of PAN nephrosis. On day 10, PAN-treated rats exhibited massive proteinuria, decreased serum albumin, and increased serum cholesterol (Table I). On day 35, these parameters were not significantly different between PAN-treated rats and controls. We detected no significant changes in serum creatinine in PAN-treated rats compared with that in controls.

No obvious macroscopic changes (Fig 1, *A*) but footprocess effacement on electron microscopy (Fig 1, *B*) of visceral GECs were observed on day 10 in PAN-treated rats. We detected no structural abnormalities on day 35 in the glomeruli of PAN-treated rats on light and electron microscopy (Fig 1, *C* and *D*).

Expression of NDST-1 mRNA in PAN nephrosis. To examine the expression of NDST-1 mRNA in pooled glomeruli, we performed Northern blotting. Glomerular expression of NDST-1 mRNA was observed as a single transcript of 8.5 kb. In PAN-treated rats, the expression of NDST-1 mRNA was reduced on day 10 (Fig 2, *A*). Densitometric analyses of the autoradiographs from 3 independent series of experiments showed that the ratios of NDST-1 mRNA against GAPDH mRNA in PAN-treated rats were significantly decreased, to 48% ± 6% of those in controls (Fig 2, *B*). On day 35, the expression of NDST-1 mRNA in the glomeruli of PAN-treated rats was 85% ± 10% of those in controls (Fig 2, *C* and *D*).

Immunofluorescence studies. Because Northern-blot analysis and examination of urine and blood as described above indicated that the decrease in expression of NDST-1 mRNA was correlated with the appearance of significant proteinuria, we sought to determine whether changes of *N*-sulfation of GAG chains occurred in the kidney. Frozen sections of renal tissue were analyzed under immunofluorecence microscopy with the specific antibody against *N*-sulfated glucosamine–enriched portion of heparan sulfate, 10E4.[25] Control rats showed well-stained GBM, Bowman's capsule, and tubular basement membrane (Fig 3, *B*), consistent with the earlier report.[25] In PAN-treated rats, we detected a significant decrease in staining in GBM on day 10, whereas the intensity of staining was not changed in other parts of the renal sections, including Bowman's capsule and tubular basement membrane (Fig 3, *A*). When we analyzed the sections with the antibody against agrin,[26] staining intensity was not changed in either group on day 10 (Fig 3, *C* and *D*). On day 35, PAN-treated rats showed intensity of staining of 10E4 on GBM similar to that in controls (data not shown). Semiquantitative analysis of staining intensity in GBM showed significant decrease of *N*-sulfated portion of heparan sulfate in PAN-treated rat GBM on day 10 compared with those in the saline solution–treated control (1.48 ± 0.11 vs 2.68 ± 0.13, $P < .05$; Table II).

Expression of NDST-1 mRNA in cultured GECs and GMCs. To further investigate the decrease in the glomerular expression of NDST-1 mRNA in PAN nephrosis rats, we studied the expression of NDST-1 mRNA in cultured GECs and GMCs. The expression of NDST-1 mRNA was 2.7 times greater in GECs than in GMCs in cells cultured for 24 hours with medium alone ($n = 3$; Fig 4).

In the next set of experiments, we studied the effect

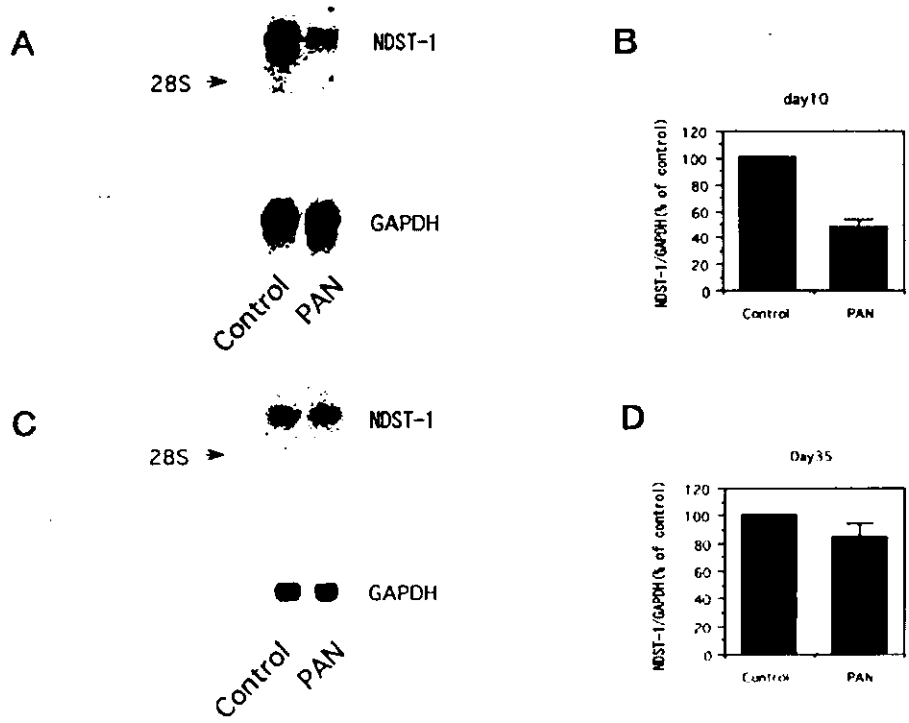

Fig 2. Northern-blot analysis for glomerular expression of NDST-1 mRNA. Northern blotting was performed with total RNA isolated on (A) day 10 or (C) day 35 from the glomeruli of PAN-treated rats or rats injected with saline solution alone. Specific probes for rat NDST-1 or GAPDH were used as described in the Methods. Densitometric analysis showed the decrease in expression of NDST-1 mRNA on day 10 in PAN-treated rats compared with that in rats injected with saline solution alone (B). Only minor differences in the expression of NDST-1 mRNA were observed on day 35 between PAN-treated rats and rats injected with saline solution alone (D). The ratio of NDST-1 mRNA against GAPDH mRNA in controls is denoted by 100%. Data expressed as mean ± SD of 3 independent experiments.

of PAN on the expression of NDST-1 mRNA by cultured GECs. Incubation of GECs for 24 hours in the presence of 50 ng/mL PAN resulted in a significant decrease in the expression of NDST-1 mRNA compared with that in controls ($n = 3$; Fig 5). Densitometric analysis revealed that the ratio of the expression of NDST-1 mRNA against GAPDH mRNA in GECs incubated for 24 hours in the presence of PAN was 67% ± 12% of that in controls ($P < .05$). The ratio in GECs cultured for 3 hours with 50 ng/mL PAN was 89% ± 17% of those in controls. GECs incubated for 24 hours with medium alone showed an increase in expression of NDST-1 mRNA compared with that in cells incubated for 3 hours with medium (Fig 5). In dose-response experiments, GECs were incubated for 24 hours with different concentrations of PAN. The expression of NDST-1 mRNA in GECs decreased significantly in a dose-dependent manner ($n = 3$; Fig 6). GEC death was not observed in this range during the experiments.

Because GMCs expressed less NDST-1 mRNA than did GECs, we performed real-time PCR to assess NDST-1 mRNA levels in GMCs. In contrast with GECs, GMCs incubated with PAN for 24 hours showed no significant decrease in the expression of NDST-1 mRNA ($n = 3$; Fig 7).

DISCUSSION

The findings of previous studies have indicated that the anionic charge in GBM is located predominantly in sulfate groups of GAG chains in HSPG.[12,39] *N*-sulfation catalyzed by NDSTs is the first and essential step in the enzymatic reactions for the sulfations of heparan sulfate GAG chain.[17,18,40,41]

Recently some heparan sulfate sulfotransferases, including 4 isozymes of NDST and 2-,3-,6-O-sulfotransferases were cloned.[20,21,28,42–45] NDST is a key enzyme that plays a pivotal role in the sulfation pathway in heparan sulfate GAG chain synthesis. Isozymes of NDST, NDST-1 (rat liver),[28] NDST-2 (murine mastocytoma),[42] NDST-3 (human brain),[20] and NDST-4 (hu-

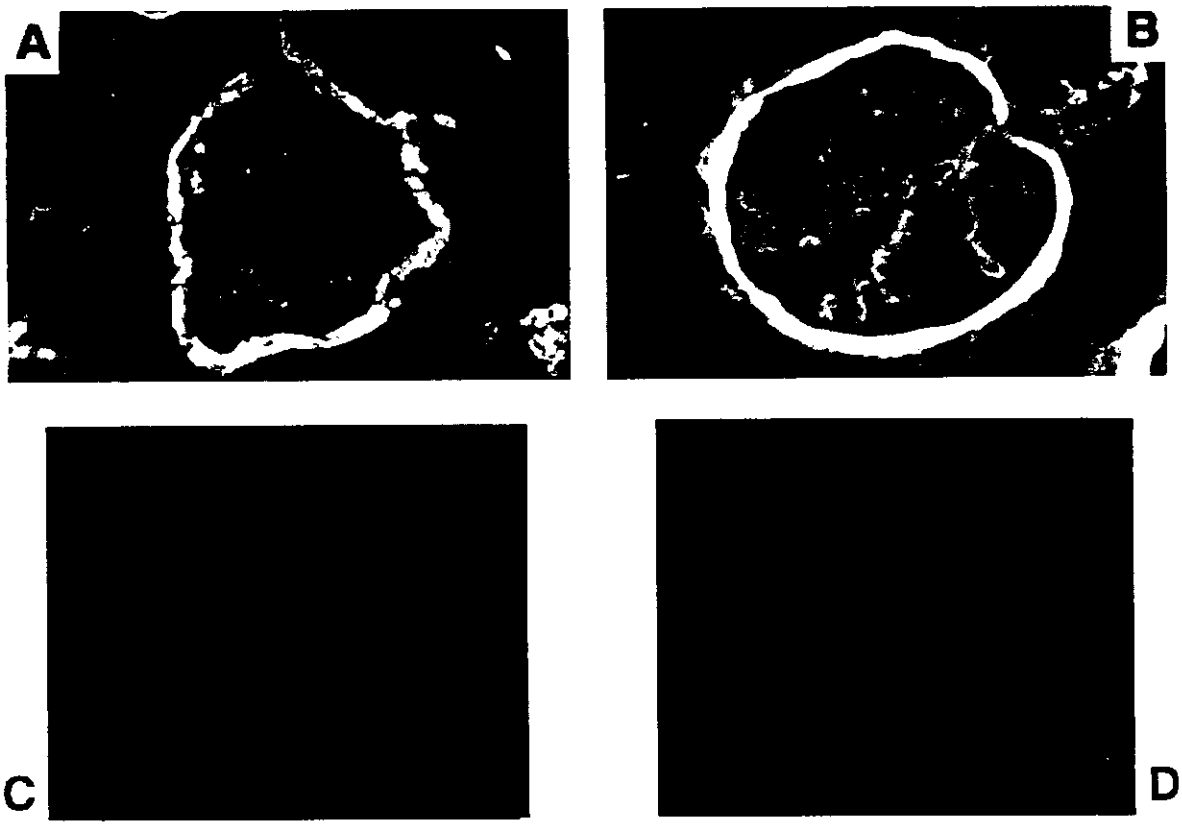

Fig 3. Immunohistochemical studies. We detected *N*-sulfated glucosamine-enriched portions of heparan sulfate and core protein agrin on frozen sections of renal tissues using specific antibodies — F58-10E4 (**A** and **B**) and MI90 (**C** and **D**), respectively (original magnification 200×). On day 10 after injection of saline solution (*B*), staining of GBM, Bowman's capsule, and tubular basement membrane by 10E4 was clear. In PAN-treated rats (*A*), the staining intensity of 10E4 on GBM was apparently decreased on day 10. We detected no differences in staining by M190 on day 10 in PAN-treated rats (*C*) and rats injected with saline solution (*D*).

Table II. Semiquantitative analysis of immunofluorescence staining

Treatment group	*N*-sulfated portion of heparan sulfate (10E4)	Agrin (MI90)
PAN		
Day 10	1.48 ± 0.11*	1.61 ± 0.36
Day 35	2.46 ± 0.15	ND
Saline solution		
Day 10	2.68 ± 0.13	1.67 ± 0.25
Day 35	2.58 ± 0.15	ND

The intensity of staining for 10E4 and agrin in GBM of each glomerulus was scored semiquantitatively, as described in the Methods section.
Data expressed as mean ± SD (n = 5).
*$P < .05$ vs controls at each time point. *ND* = not determined.

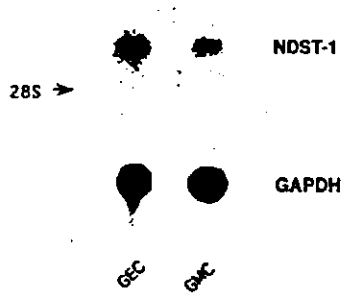

Fig 4. Expression of NDST-1 mRNA in cultured GECs and GMCs. Northern-blot analysis was performed with total RNA isolated from the cells incubated for 24 hours with the media as described in the Methods.

man and mouse cDNA library)[21] have been identified, but their distribution and relative contribution in heparan sulfate synthesis in certain tissues are largely unknown. Aikawa and Esko[20,21] reported that NDST-1, -2, and -3 are expressed in human kidney, but the contribution of each isozyme to heparan sulfate sulfa-

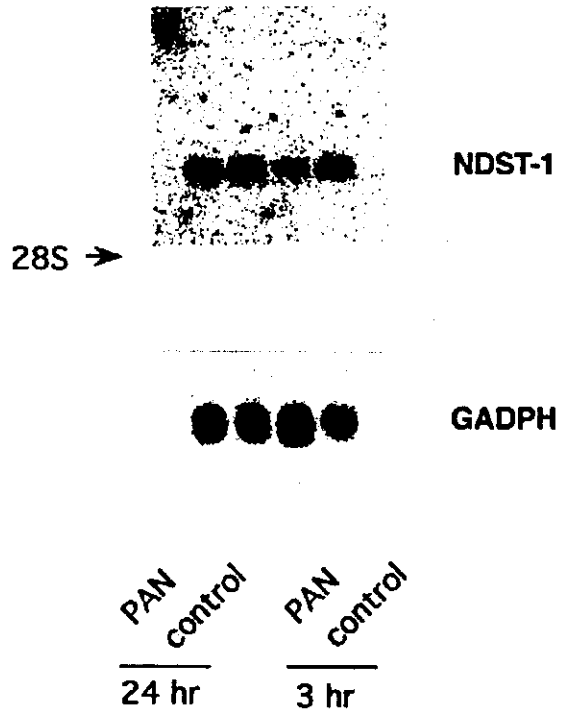

Fig 5. Effect of PAN on expression of NDST-1 mRNA in cultured GECs. Northern-blot analysis was performed with total RNA isolated from GECs incubated for 3 or 24 hours in the presence of 50 ng/mL PAN as described in the Methods section.

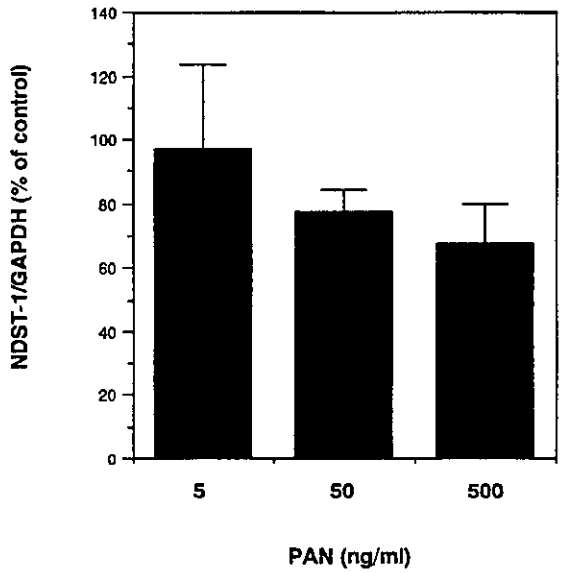

Fig 6. Summary of Northern-blot analyses in dose-response experiments in GECs. GECs were incubated for 24 hours in the presence of PAN at concentrations of 5, 50, and 500 ng/mL. The percentages of the ratio of NDST-1 mRNA expression were calculated relative to the ratio in controls as described in the Methods. The ratio of the expression of NDST-1 mRNA against GAPDH mRNA in controls is indicated by 100%. Data expressed as mean ± SD of 3 independent experiments.

tion in the glomeruli remains to be elucidated. Our data suggest that NDST-1 activity is involved in the sulfation of HS in glomeruli, consistent with a recent report in NDST-1–knockout mice.[46]

In this study, we demonstrated that glomerular expression of NDST-1 mRNA in PAN-treated rats was decreased at the nephrotic phase. The reduction in the level of NDST-1 mRNA was accompanied by a loss of *N*-sulfated GAG chains of HSPG in GBM without changes in core protein agrin, suggesting a decrease in NDST activity. Furthermore, the disappearance of significant proteinuria corresponded with the return to normal expression of NDST-1 mRNA in glomeruli and of *N*-sulfated GAG chains in GBM.

These results indicate that a disturbance of enzymatic reaction for sulfations in GAG chains of HSPG plays an important role in the mechanism of significant proteinuria in the PAN nephrosis model; the authors of recent studies have reported that changes in cell-surface sialoglycoproteins (eg, podocalyxin and podoplanin) or foot process–associated molecules (including nephrin and podocin on podocytes) are also involved in the development of proteinuria in this animal model.[47–49] Furthermore, our results are consistent with those from other studies demonstrating that the injection of specific antibodies against the heparan sulfate GAG side chain of HSPG induces proteinuria, probably by masking anionic charge in the heparan sulfate GAG side chain,[14] whereas antibodies against the core protein of HSPG do not cause proteinuria.[50]

In this study, the changes in glomerular expression of NDST-1 and *N*-sulfated GAG chains were assessed at a limited number of time points. To determine clearly the causality of alterations of the heparan sulfate sulfation pathway to proteinuria in PAN nephrosis, further investigation at multiple time points, especially earlier ones, is needed.

Several reports suggest a role for ROS in PAN nephrosis.[51,52] Raats and Berden[19] reported that heparan sulfate side chains of rat agrin were depolymerized in vitro by ROS and suggest that ROS can affect the permeability of the GBM by way of heparan sulfate depolymerization. It may be that the decrease in NDST-1 in glomeruli impaired the repair process for the heparan sulfate initially damaged by ROS in GBM, leading to massive proteinuria.

We also demonstrated in this study that GECs expressed more NDST-1 mRNA than GMCs, a finding in agreement with the results of recent in vitro studies showing that GECs synthesize more HSPG than do

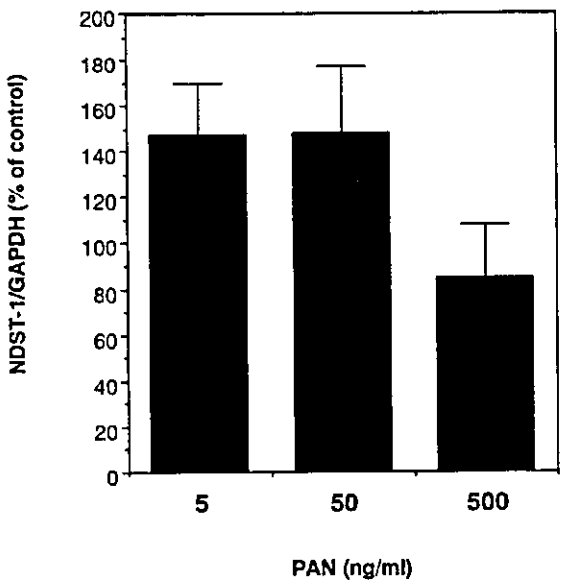

Fig 7. Summary of real-time PCR in dose-response experiments in GMCs. GMCs were incubated for 24 hours in the presence of PAN at concentrations of 5, 50, and 500 ng/mL. The percentages of the ratio of NDST-1 mRNA expression were calculated relative to the ratio in controls as described in the Methods section. The ratio of the expression of NDST-1 mRNA against GAPDH mRNA in controls is denoted by 100%. Data expressed as mean ± SD of 3 independent experiments.

GMCs as detected on ELISA with a specific antibody against heparan sulfate GAG side chain in HSPG.[53] The incubation of GECs with PAN reduces the expression of NDST-1 mRNA in a time- and dose-dependent manner. We used PAN in culture at concentrations ranging from 5 to 500 ng/mL; no GEC death was observed in this range during the experiments. It has been shown that the concentration of PAN capable of inducing general toxicity is at least 10 μg/mL.[34,54] In addition, the production of the core protein of HSPG in GECs is known to be unaltered in the presence of PAN at a concentration less than 50 μg/mL.[55] Thus the results showed that NDST-1 is involved in the assembly of heparan sulfate in GEC, and suggests that GECs, rather than GMCs, contribute to the glomerular disturbance of *N*-sulfation of heparan sulfate after administration of PAN, without the change of HSPG core protein, including agrin.

Taken together, our results show for the first time, to our knowledge, that transcriptional alteration of the glomerular NDST-1 occurs at a nephrotic phase in PAN nephrosis. We suggest that the alteration of NDST-1 mRNA in glomeruli is associated with the reduction of *N*-sulfated GAG chains of HSPG on GBM and contributes at least somewhat to the mechanism of proteinuria in the PAN nephrosis model. Because a previous report indicated that GEC is the major target of PAN in PAN nephrosis,[56] it may be that the transcriptional decrease of NDST-1 in GEC contributes to the undersulfation of heparan sulfate in GBM and proteinuria in PAN nephrosis.

We thank Professor Mohamed R. Daha, Professor Leendert A. van Es and Dr Emile de Heer for their critical review of this paper.

REFERENCES

1. Chang RLS, Deen WM, Robertson CR, Brenner BM. Permselectivity of the glomerular capillary wall. III. Restricted transport of polyanions. Kidney Int 1975;8:212-8.
2. Brenner BM, Hostetter TH, Humes HD. Molecular basis of proteinuria of glomerular origin. N Engl J Med 1978;298:826-833.
3. Guasch A, Deen WM, Myers BD. Charge selectivity of the glomerular filtration barrier in healthy and nephrotic humans. J Clin Invest 1993;92:2274-82.
4. Kanwar YS. Biophysiology of glomerular filtration and proteinuria. Lab Invest 1984;51:7-21.
5. Remuzzi A, Remuzzi G. Glomerular perm-selective function. Kidney Int 1994;45:398-402.
6. Kitano Y, Yoshikawa N, Nakamura H. Glomerular anionic sites in minimal change nephrotic syndrome and focal segmental glomerulosclerosis. Clin Nephrol 1993;40:199-204.
7. Kanwar YS, Farquhar MG. Presence of heparan sulfate in the glomerular basement membrane. Proc Natl Acad Sci U S A 1979;76:1303-7.
8. Kerjaschki D, Sharkey DJ, Farquhar MG. Identification and characterization of podocalyxin — the major sialoprotein of the renal glomerular epithelial cell. J Cell Biol 1984;98:1591-8.
9. Stow JL, Sawada H, Farquhar MG. Basement membrane heparan sulfate proteoglycans are concentrated in the lamina rarae and in podocytes of the rat renal glomerulus. Proc Natl Acad Sci U S A 1985;82:3296-300.
10. Kanwar YS, Linker A, Farquhar MG. Increased permeability of the glomerular basement membrane to ferritin after removal of glycosaminoglycans (heparan sulfate) by enzyme digestion. J Cell Biol 1980;86:688-93.
11. Tamsma JT, van den Born J, Bruijn JA, Assmann KJM, Weening JJ, Berden JHM, et al. Expression of glomerular extracellular matrix components in human diabetic nephropathy: decrease of heparan sulfate in the glomerular basement membrane. Diabetologia 1994;37:313-20.
12. van der Woude FJ, van Det NF. Heparan sulfate proteoglycans and diabetic nephropathy. Exp Nephrol 1997;5:180-8.
13. van den Born J, van den Heuvel LPWJ, Bakker MAH, Veerkamp JH, Assmann KJM, Weening JJ, et al. Distribution of GBM heparan sulfate proteoglycan core protein and side chains in human glomerular diseases. Kidney Int 1987;43:454-63.
14. van den Born J, van den Heuvel LPWJ, Bakker MAH, Veerkamp JH, Assmann KJM, Berden JHM. A monoclonal antibody against GBM heparan sulfate induces an acute selective proteinuria in rats. Kidney Int 1992;41:115-23.
15. Caulfield JP, Farquhar MG. Loss of anionic sites from the glomerular basement membrane in aminonucleoside nephrosis. Lab Invest 1978;39:505-12.
16. Olson JL, Rennke HG, Venkatachalam MA. Alterations in the charge and size selectivity barrier of the glomerular filter in aminonucleoside nephrosis in rats. Lab Invest 1981;44:271-9.
17. Brandan E, Hirschberg CB. Purification of rat liver *N*-heparan sulfate sulfotransferase. J Biol Chem 1988;263:2417-22.
18. Bame KJ, Esko JD. Undersulfated heparan sulfate in a Chinese hamster ovary cell mutant defective in heparan sulfate *N*-sulfotransferase. J Biol Chem 1989;264:8059-65.

19. Raats CJI, van den Born J, Berden JHM. Glomerular heparan sulfate alterations: mechanisms and relevance for proteinuria. Kidney Int 2000;57:385-400.
20. Aikawa J, Esko JD. Molecular cloning and expression of a third member of the heparan sulfate/heparin GlcNAc *N*-deacetylase/*N*-sulfotransferase family. J Biol Chem 1999;274:2690-5.
21. Aikawa J, Grobe K, Tsujimoto M, Esko JD. Multiple isozymes of heparan sulfate/heparin GlcNAc N-deacetylase/GlcN N-sulfotransferase. Structure and activity of the fourth member, NDST4. J Biol Chem 2001;276:5876-82.
22. Frenk S, Antonowicz I, Craig JM, Metcoff J. Experimental nephrotic syndrome induced in rats by aminonucleoside. Renal lesion and body electrolyte composition. Proc Soc Exp Biol Med 1955;89:424-7.
23. Striker GE, Killen PD, Farin FM. Human glomerular cells in vitro: isolation and characterization. Transplant Proc 1980;12:88-99.
24. Lee LK, Pollock AS, Lovett DH. Asymmetric origins of the mature glomerular basement membrane. J Cell Physiol 1993;157:169-77.
25. David G, Bai XM, van der Schueren B, Cassiman JJ, van den Berghe H. Developmental changes in heparan sulfate expression: in situ detection with mAbs. J Cell Biol 1992;119:961-75.
26. Raats CJI, Bakker MAH, Hoch W, Tamboer WPM, Groffen AJA, van den Heuvel LPWJ, et al. Differential expression of agrin in renal basement membranes as revealed by domain-specific antibodies. J Biol Chem 1998;273:17832-8.
27. Groffen AJ, Ruegg MA, Dijkman HBPM, van den Verden TJ, Buskens CA, van den Born J, et al. Agrin is a major heparan sulfate proteoglycan in the human glomerular basement membrane. J Histochem Cytechem 1998;46:19-27.
28. Hashimoto Y, Orellana A, Gil G, Hirschberg CB. Molecular cloning and expression of rat liver *N*-heparan sulfate sulfotransferase. J Biol Chem 1992;267:15744-50.
29. Fort Ph, Marty L, Piechaczyk H, El Sabrouty S, Dani C, Jeanteur Ph, et al. Various rat adult tissues express only one major mRNA species from the glyceraldehyde-3-phosphate dehydrogenase multigenic family. Nucleic Acids Res 1985;13:1431-42.
30. Natori Y, Igawa Y, Nakao N, Natori Y. Cytotoxicity of sera from rats with puromycin aminonucleoside nephrosis. Nephron 1996; 73:258-63.
31. Natori Y, Hayakawa I, Shibata S. Passive Heymann nephritis with acute and severe proteinuria induced by heterologous antibody against renal tubular brush border glycoprotein gp108. Lab Invest 1986;55:63-70.
32. Ootaka T, Suzuki M, Sudo K, Sato H, Seino J, Saito T, et al. Histologic localization of terminal complement complexes in renal diseases. Am J Clin Pathol 1989;91:144-51.
33. Sato H, Saito T, Seino J, Ootaka T, Kyogoku Y, Furuyama T, et al. Dense deposit disease, its possible pathogenesis suggested by an observation of a patient. Clin Nephrol 1987;27:41-5.
34. Yamabe H, Yoshikawa S, Ohsawa H, Inuma H, Miyata M, Sasaki T, et al. Tissue factor production by cultured rat glomerular epithelial cells. Nephrol Dial Transplant 1993;8:519-23.
35. Natori Y, Natori Y, Nishimura T, Yamabe H, Iyonaga K, Takeya M, et al. Production of monocyte chemoattractant protein-1 by cultured glomerular epithelial cells: inhibition by dexamethasone. Exp Nephrol 1997;5:318-22.
36. Natori Y, O'Meara YM, Manning EC, Minto AWM, Levine JS, Weise WJ, et al. Production and polarized secretion of basement membrane components by glomerular epithelial cells. Am J Physiol 1992;262:F131-7.
37. Harper CA, Robinson JM, Hoover RL, Wright TC, Karnovsky MJ. Improved methods for culturing rat glomerular cells. Kidney Int 1984;26:875-80.
38. Chomczynski P, Sacchi N. Single step method of RNA isolation by acid–guanidine thiocyanate–phenol–chloroform extraction. Anal Biochem 1987;162:156-9.
39. Kjellen L, Lindahl U. Proteoglycan: structure and interactions. Annu Rev Biochem 1991;60:443-75.
40. Ishihara M, Guo Y, Wei Z, Yang Z, Swiedler SJ, Orellana A, et al. Regulation of biosynthesis of the basic fibroblast growth factor binding domains of heparan sulfate by heparan sulfate-*N*-deacetylase/*N*-sulfotransferase expression. J Biol Chem 1993;268:20091-5.
41. Lindahl U, Lidholt K, Spillmann D, Kjellen L. More to "heparin" than anticoagulation. Thrombosis Res 1994;75:1-32.
42. Orellana A, Hirschberg CB, Wei Z, Swiedler SJ, Ishihara M. Molecular cloning and expression of a glycosaminoglycan *N*-acetylglucosaminyl *N*-deacethylase/*N*-sulfotransferase from a heparin-producing cell line. J Biol Chem 1994;269:2270-6.
43. Shworak NW, Liu J, Fritze LM, Schwartz JJ, Zhang L, Logeart D, et al. Molecular cloning and expression of mouse and human cDNAs encoding heparan-sulfate D-glucosaminyl 3-O-sulfotransferase. J Biol Chem 1997;272:28008-19.
44. Habuchi H, Kobayashi M, Kimata K. Molecular characterization and expression of heparan-sulfate 6-sulfotransferase. Complete cDNA cloning in human and partial cloning in Chinese hamster ovary cells. J Biol Chem 1998;273:9208-13.
45. Kobayashi M, Habuchi H, Yoneda M, Habuchi O, Kimata K. Molecular cloning and expression of Chinese hamster ovary cell heparan-sulfate 2-sulfotransferase. J Biol Chem 1997;272:13980-5.
46. Ringvall M, Ledin J, Holmborn K, van Kuppevelt T, Ellin F, Eriksson I, et al. Defective heparan sulfate biosynthesis and neonatal lethality in mice lacking *N*-deacetylase/*N*-sulfotransferase-1. J Biol Chem 2000;275:25926-30.
47. Kerjaschki D, Vernillo AT, Farquhar MG. Reduced sialylation of podocalyxin — the major sialoprotein of the rat kidney glomerulus — in aminonucleoside nephrosis. Am J Pathol 1985;118:343-9.
48. Breiteneder-Geleff S, Matsui K, Soleiman A, Meraner P, Poczewski H, Kalt R, et al. Podoplanin, novel 43-kd membrane protein of glomerular epithelial cells, is down-regulated in puromycin nephrosis. Am J Pathol 1997;151:1141-52.
49. Kawachi H, Koike H, Kurihara H, Yaoita E, Orikasa M, Shia MA, et al. Cloning of rat nephrin: expression in developing glomeruli and in proteinuric states. Kidney Int 2000;57:1949-61.
50. Makino H, Gibbons JT, Kumudavalli Reddy M, Kanwar YS. Nephritogenicity of antibodies to proteoglycans of the glomerular basement membrane-1. J Clin Invest 1986;77:142-56.
51. Diamond JR, Bonventre JV, Karnovsky MJ. A role for oxygen free radicals in aminonucleoside nephrosis. Kidney Int 1986;29:478-83.
52. Gwinner W, Landmesser U, Brandes RP, Kubat B, Plasger J, Eberhard O, et al. Reactive oxygen species and antioxidant defense in puromycin aminonucleoside glomerulopathy. J Am Soc Nephrol 1997;8:1722-31.
53. van Det NF, van den Born J, Tamsma JT, Verhagen NAM, van den Heuvel LPWJ, Berden JHM, et al. Proteoglycan production by human glomerular visceral epithelial cells and mesangial cells in vitro. Biochem J 1995;307:759-68.
54. Fishman JA, Karnovsky MJ. Effects of the aminonucleoside of puromycin on glomerular epithelial cells in vitro. Am J Pathol 1985;118:398-407.
55. Kasinath BS, Singh A, Kanwar YS, Lewis EJ. Effect of puromycin aminonucleoside on HSPG core protein content of glomerular epithelial cells. Am J Physiol 1988;255:F590-6.
56. Ryan GB, Karnovsky MJ. An ultrastructural study of the mechanisms of proteinuria in aminonucleoside nephrosis. Kidney Int 1975;8:219-32.

Kidney International, Vol. 65 (2004), pp. 2228–2237

Role of mast cells in the development of renal fibrosis: Use of mast cell–deficient rats

SHINOBU MIYAZAWA, OSAMU HOTTA, NAOKO DOI, YUMIKO NATORI, KIYOTAKA NISHIKAWA, and YASUHIRO NATORI

Department of Clinical Pharmacology, Research Institute, International Medical Center of Japan, Tokyo, Japan; Department of Nephrology, Sendai Shakaihoken Hospital, Sendai, Japan

Role of mast cells in the development of renal fibrosis: Use of mast cell–deficient rats.

Background. Recent clinical studies have shown that the number of interstitial mast cells increases in various types of renal disease and correlates well with the magnitude of interstitial fibrosis. The present study was conducted to assess the role of mast cells in renal fibrosis by examining an experimental glomerular disease.

Methods. A rat model of chronic glomerular disease, puromycin aminonucleoside-nephrosis, was induced in mast cell–deficient (*Ws/Ws*) and normal (+/+) rats.

Results. The area of interstitial fibrosis was widely distributed at 6 weeks in both groups of rats; however, unexpectedly, the area of interstitial fibrosis was greater in *Ws/Ws* rats than in +/+ littermates. Biochemical analysis of the hydroxyproline content confirmed the more severe fibrosis in the *Ws/Ws* rats. The number of mast cells increased in both *Ws/Ws* and +/+ rats, concomitant with the development of interstitial fibrosis, but was confirmed to be lower in *Ws/Ws* than in +/+ rats. There were no differences in the numbers of interstitial macrophages and T lymphocytes between the two groups. Reverse transcription-polymerase chain reaction analysis of cytokine expression revealed that the level of mRNA for transforming growth factor-β (TGF-β), a potent profibrotic cytokine, was higher in *Ws/Ws* rats. In addition, heparin, one of the major components of mast cells, inhibited the expression of TGF-β mRNA in rat fibroblasts in culture.

Conclusion. These results suggest that mast cells do not play a major role in the pathogenesis of interstitial fibrosis in puromycin aminonucleoside nephrosis. Rather, they might be protective or ameliorative in this model through the inhibition of TGF-β production by heparin, and possibly in other models and also in humans.

Mast cells are known to be immune-effector cells that augment inflammatory reactions. It is widely accepted that mast cells are involved in a number of allergic inflammatory diseases as well as in host defense against pathogens. In addition, several lines of evidence suggest that mast cells may participate in fibrotic processes. Mast cells are found in fibrogenic lesions in various tissues in human diseases, such as pulmonary fibrosis [1, 2], hepatic cirrhosis [3, 4], scleroderma [5, 6], and keloid [7]. Mast cells serve as a rich source of several mediators [8], including histamines, proteoglycans, and proteolytic enzymes (proteases), as well as a number of cytokines [9], some of which are reported to be mitogenic [10] and chemotactic [11] for fibroblasts, and to stimulate the production of the extracellular matrix (ECM) by fibroblasts [9, 10, 12]. Furthermore, mast cells themselves produce components of the ECM [13]. Therefore, for these reasons they are considered to play a profibrogenic role in the above-mentioned diseases.

In recent years, mast cells were shown to be present in the interstitial area of human renal biopsy tissues from patients with various renal diseases, such as IgA nephropathy [14–16], rapidly progressive glomerulonephritis [17], focal and segmental glomerulosclerosis [15], diabetic nephropathy [15, 18], and kidney graft rejection [16, 19, 20]. Furthermore, the number of interstitial mast cells in these glomerular diseases correlates well with the degree of interstitial fibrosis. Tubulointerstitial lesions including interstitial fibrosis are considered to be prognostic features of various glomerular diseases; regardless of its primary causes, decreased renal function correlates most closely with pathologic changes in the tubulointerstitium, which include interstitial fibrosis, tubular atrophy, and loss of peritubular capillaries [21, 22]. Based on these observations, mast cells are suggested to contribute to the renal deterioration in glomerular diseases by inducing interstitial fibrosis [14, 15, 17]. However, there have been no studies that directly show the involvement of mast cells in the pathogenesis of interstitial fibrosis in the kidney.

To elucidate the role of mast cells in the interstitial fibrosis in progressive glomerular diseases, we

Key words: mast cell, *Ws/Ws rat*, renal fibrosis, animal model, transforming growth factor-β.

Received for publication January 26, 2003
and in revised form September 5, 2003, and December 11, 2003
Accepted for publication January 15, 2004

© 2004 by the International Society of Nephrology

investigated the accumulation of mast cells in an animal model of glomerular disease that is accompanied by interstitial fibrosis and renal deterioration. Furthermore, we utilized mast cell–deficient *Ws/Ws* rats to test if mast cells contribute to the development of the interstitial fibrosis. *Ws/Ws* rats have very few mast cells in their skin and other tissues [less than 1% of the number in control (+/+) littermates] because of a small deletion in the tyrosine kinase domain of the *c-kit* gene [23–25]. Unexpectedly, in this study we found that the degree of interstitial fibrosis was more severe in *Ws/Ws* rats than in the control littermates, suggesting that mast cells do not contribute to the development of interstitial fibrosis in this model. Rather, they may actually play a beneficial role in the process of fibrosis in the kidney.

METHODS

Animal model

Puromycin aminonucleoside (PAN) nephrosis model was induced in male mast cell–deficient *Ws/Ws* and their normal +/+ littermates (Japan SLC; Hamamatsu, Japan, $N = 12$ each), weighing 140 to 160 g, by the method of Jones et al [26], with slight modifications. In brief, left unilateral nephrectomy through a flank incision was performed on each rat under sodium pentobarbital (45 mg/kg body weight) anesthesia. Five days after the nephrectomy, the rats received an intraperitoneal (i.p.) injection of PAN (Sigma Chemical Co., St. Louis, MO, USA) dissolved in 0.9% saline (15 mg/mL) and given at a dose of 15-mg/100 g body weight. Second, third, and fourth doses of PAN (4.3 mg/100 g body weight, i.p.) were administered at 3, 4, and 5 weeks, respectively, after the initial dose. Control animals did not receive any surgical procedures or injections ($N = 10$ each). All animals were maintained on a standard rat diet and had free access to water throughout the course of the experiment. The animals were housed individually in metabolic cages to obtain 24-hour urine once every week. They were sacrificed sequentially at 2 ($N = 5$ each) and 6 weeks ($N = 5$ each except for $N = 4$ for PAN-injected *Ws/Ws* rats; see below) after the initial dose of PAN, namely, 1 week after the first and the last injections, respectively. Three of the PAN-injected *Ws/Ws* rats and 2 of the PAN-injected +/+ rats died of chronic renal failure by 6 weeks. These rats were found dead in their cages in the morning, and thus their kidneys could not be used for histologic studies. These animals were excluded from the subsequent analysis. At sacrifice, blood samples were collected by heart puncture under anesthesia with diethylether. The kidneys were perfused via the abdominal aorta with ice-cold saline, and pieces of renal tissues were fixed in 10% buffered formalin or periodate-lysine-paraformaldehyde (PLP) solution. Pieces of renal cortex were also used for RNA preparation and hydroxyproline analysis (see below). Urinary protein was quantified by the biuret method. Levels of blood urea nitrogen (BUN) were measured with a kit designed for clinical use (Wako Pure Chemical Industries, Osaka, Japan).

Kidney tissue preparation

The kidney tissues fixed in 10% buffered formalin were embedded in paraffin, sectioned, and stained with hematoxylin and eosin, periodic acid-Schiff (PAS), or Masson trichrome. The degree of interstitial fibrosis was semiquantitatively analyzed by inspection of Masson trichrome–stained sections and graded on a scale of 0 to 3 as follows: (*0*), no apparent damage; (*1*) mild damage, with lesions involving less than 5% of the cortex; (*2*) moderate damage, involving 5% to 20% of the cortex; and (*3*) severe damage, involving more than 20% of the cortex. Pieces for cryostat sectioning were fixed in PLP solution for 4 hours, washed several times in phosphate-buffered saline (PBS) containing 7% sucrose, embedded in Tissue-Tek OCT compound (Sakura Finetek, Torrance, CA, USA), and snap-frozen.

Immunohistochemical study

To block endogenous peroxidase activity, we treated sections of frozen or paraffin-embedded kidney tissues with methanol containing 0.6% hydrogen peroxide for 15 minutes and then washed them with PBS. They were stained by the standard avidin-biotin peroxidase technique with sheep antirat mast cell protease (RMCP) I (mast cell–specific antibody; Moredun, Scotland, UK), mouse monoclonal antibody ED-1 (specific for rat monocytes/macrophages), W3/25 ($CD4^+$ cells), or OX8 ($CD8^+$ cells) at 4°C overnight. The sections were incubated with the corresponding second antibodies, biotinylated donkey antisheep IgG or horse antimouse IgG, and stained with the reagents of an ABC staining kit (Vector Laboratories, Inc., Burlingame, CA, USA). Sections were also stained with horseradish peroxidase–conjugated mouse antihuman α-smooth muscle actin (α–SMA, a marker for myofibroblasts) monoclonal antibody (Dako Corp., Carpinteria, CA, USA). All sections were then developed with 3, 3′-diaminobenzidine solution as chromogen and counterstained with methylgreen. With the aid of a 10 × 10 eyepiece grid, the numbers of monocytes/macrophages, $CD4^+$, and $CD8^+$ cells in the interstitium were counted manually in 6 random nonoverlapping cortical fields (×400) of sections made from each experimental animal. RMCP I–positive interstitial mast cells were also counted in 20 random cortical fields (×100). The results of cell counting were expressed as the number per square millimeter.

Cell cultures

A cell line of renal fibroblasts (NRK49F) derived from rat kidney was obtained from The European